



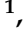




## Article

# Distinguishing between Sources of Natural Dissolved Organic Matter (DOM) Based on Its Characteristics

Rolf David Vogt <sup>1,\*</sup> , Petr Porcal <sup>2</sup> , Ma. Cristina Paule-Mercado <sup>2</sup> , Ståle Haaland <sup>3,4</sup> , Cathrine Brecke Gundersen <sup>1</sup> , Geir Inge Orderud <sup>5</sup>  and Bjørnar Eikebrokk <sup>6</sup> 

<sup>1</sup> Norwegian Institute for Water Research, 0579 Oslo, Norway; cathrine.brecke.gundersen@niva.no

<sup>2</sup> Biology Centre, Academy of Sciences of the Czech Republic (CAS), Institute of Hydrobiology, 370 05 České Budějovice, Czech Republic; porcal@hbu.cas.cz (P.P.); hejzlar@hbu.cas.cz (J.H.); cristina.mercado@hbu.cas.cz (M.C.P.-M.)

<sup>3</sup> Norwegian Institute of Bioeconomy Research, Division of Environment and Natural Resources, 1431 Ås, Norway; staale.haaland@nmbu.no

<sup>4</sup> Faculty of Environmental Sciences and Natural Resource Management, Norwegian University of Life Sciences, 1433 Ås, Norway

<sup>5</sup> Norwegian Institute for Urban and Regional Research, Oslo Met-Oslo Metropolitan University, 0130 Oslo, Norway; geiro@oslomet.no

<sup>6</sup> Drikkevannskonsult, 7047 Trondheim, Norway; bjorneik@online.no

\* Correspondence: rolf.david.vogt@niva.no

**Abstract:** Increasing levels of dissolved organic matter (DOM) in watercourses in the northern hemisphere are mainly due to reduced acid rain, climate change, and changes in agricultural practices. However, their impacts vary in time and space. To predict how DOM responds to changes in environmental pressures, we need to differentiate between allochthonous and autochthonous sources as well as identify anthropogenic DOM. In this study we distinguish between allochthonous, autochthonous, and anthropogenic sources of DOM in a diverse watercourse network by assessing effects of land cover on water quality and using DOM characterization tools. The main sources of DOM at the studied site are forests discharging allochthonous humic DOM, autochthonous fulvic DOM, and runoff from urban sites and fish farms with high levels of anthropogenic DOM rich in protein-like material. Specific UV absorbency (sUVa) distinguishes allochthonous DOM from autochthonous and anthropogenic DOM. Anthropogenic DOM differs from autochthonous fulvic DOM by containing elevated levels of protein-like material. DOM from fishponds is distinguished from autochthonous and sewage DOM by having high sUVa. DOM characteristics are thus valuable tools for deconvoluting the various sources of DOM, enabling water resource managers to identify anthropogenic sources of DOM and predict future trends in DOM.

**Keywords:** DOM; allochthonous; autochthonous; natural; anthropogenic; sUVa; EEA indices; fractionation; PARAFAC; fishponds



**Citation:** Vogt, R.D.; Porcal, P.; Hejzlar, J.; Paule-Mercado, M.C.; Haaland, S.; Gundersen, C.B.; Orderud, G.I.; Eikebrokk, B. Distinguishing between Sources of Natural Dissolved Organic Matter (DOM) Based on Its Characteristics. *Water* **2023**, *15*, 3006. <https://doi.org/10.3390/w15163006>

Academic Editor: Gang Wen

Received: 26 July 2023

Revised: 17 August 2023

Accepted: 18 August 2023

Published: 20 August 2023



**Copyright:** © 2023 by the authors. Licensee MDPI, Basel, Switzerland. This article is an open access article distributed under the terms and conditions of the Creative Commons Attribution (CC BY) license (<https://creativecommons.org/licenses/by/4.0/>).

## 1. Introduction

Dissolved organic matter (DOM) plays a key role in governing biogeochemical processes in soft freshwater environments by supplying energy and nutrients, transporting, and effecting the toxicity of pollutants, and increasing light attenuation, and it poses a challenge for waterworks. DOM primarily originates from the terrestrial environment, known as allochthonous material [1]. However, there is also a production of DOM by algae and other aquatic plants and microorganisms [2] in the surface waters (i.e., autochthonous), particularly in eutrophic lake waters. The main moiety of natural allochthonous DOM is humic compounds, which have a relatively high aromaticity and molecular weight. On the other hand, autochthonous DOM is dominated by fulvic matter, which has lower aromaticity and size [3]. Additionally, in most watercourses, there are anthropogenic inputs of DOM. Admittedly, many of the environmental states we observe have their origin in

human societies, giving rise to theoretical approaches and models aiming at merging nature and society when analyzing those states e.g., [4–8]. Although recognizing the importance of human societies cum anthropogenic drivers when analyzing environmental states, in this paper, anthropogenic inputs of DOM in watercourses are referring to direct pollution, thereby allowing for analytically distinguishing between direct and indirect effects. Anthropogenic in this context is thus referring to local sources of DOM pollution, such as from fishponds. On this basis, it is possible to conduct more informed analyses of the interaction between natural and anthropogenic factors (human societies), moving towards some type of merged study, but doing so is far beyond the scope of this paper. The anthropogenic DOM shares some characteristics with autochthonous DOM, such as generally low specific UV absorbency and higher biodegradability compared to allochthonous DOM [9].

In recent decades, a widespread increase in browning of freshwater bodies has been observed in the northern hemisphere. This is primarily caused by an elevated flux of allochthonous DOM to rivers and lakes [10]. The main drivers behind this increase include declined sulfur deposition [11] with decreased ionic strength [12], increased biomass due to afforestation and reduced grazing [13], as well as the impacts of increased wetness of soils [14] and a warmer climate [15,16]. However, future increases in surface water DOM are expected to be driven by factors other than further declines in the deposition of sulfur [17]. These factors may include changes in biomass due to climate, re-/afforestation, other land use changes [13], and the accumulation of nitrogen deposition [18]. To predict the effects of these drivers and pressures on DOM, there is a need for better source appointment of the DOM. Additionally, our freshwater systems are recipients of direct inputs of anthropogenic DOM, making it important for environmental managers to predict future developments in DOM and identify the presence of anthropogenic DOM in watercourses. This is a wicked task due to the combination of spatiotemporal variances in the drivers and spatial differences in the role of these governing factors, causing deviations in current increases in DOM concentration.

The concentration of DOM is commonly measured using proxies such as total or dissolved organic carbon (TOC or DOC) and UV absorbency or color. In lakes with poor ecological conditions, Kaste et al. [19] observed that higher DOC levels are associated with lower relative absorbencies, reflecting that less aromatic autochthonous or anthropogenic DOM is more abundant in such lakes. A commonly used index to characterize DOM is thus the specific UV absorbency (sUVa). It is calculated by dividing the absorbance of DOM at  $\lambda_{254}$  ( $UV_{\lambda_{254}}$ ) by DOC [20], providing information regarding the degree of aromaticity of the DOM. Biological oxygen demand (BOD) and chemical oxygen demand (COD) are commonly used to measure organic pollution. BOD<sub>5</sub> reflects the portion of DOM that can be biodegraded by bacteria during a 5-day incubation, while COD measures the overall chemical oxidation potential of DOM. The ratio between BOD<sub>5</sub> and COD (BOD<sub>5</sub>/COD) indicates the relative biodegradability of the DOM. COD can be determined using either the manganese (COD<sub>Mn</sub>) or dichromate (COD<sub>Cr</sub>) oxidation methods, with COD<sub>Cr</sub> being the stronger method yielding usually between two- and five-times higher values compared to COD<sub>Mn</sub> in surface waters [2]. In raw sewage, the average BOD<sub>5</sub>/COD<sub>Cr</sub> ratio is above 0.4 [21]. Based on the understanding that allochthonous DOM has higher UV absorbency and is less biodegradable than autochthonous and anthropogenic DOM, Kaste et al. [19] hypothesized that sUVa values below 0.033 and BOD<sub>5</sub>/COD<sub>Mn</sub> values above 0.5 indicate a significant contribution of autochthonous or anthropogenic DOM.

Fluorescence indexes determined from fluorescence excitation-emission matrices (EEM) are commonly employed to further assess the spectroscopic characteristics of DOM. The humification index (HIX) is a proxy for the relative degree of humification [22], the biological index (BIX) indicates the recent autochthonous contribution, and the fluorescence index (FI) ratio distinguishes between allochthonous DOM and autochthonous DOM derived from microbial activity or protein-like material associated with anthropogenic DOM from sewage [23]. These spectroscopic indexes thus provide information about the relative proportions of autochthonous, allochthonous, and anthropogenic humic matter

within the DOM. EEM data are furthermore analyzed using parallel factor (PARAFAC) analysis [24], which allows for the distinct appointment of the humic allochthonous, fulvic autochthonous, and protein-like anthropogenic components within the DOM material [25].

Hydrophobic and hydrophilic acid, bases, and neutral moieties of the DOM are commonly determined by tandem solid phase extraction. Allochthonous DOM is generally found to contain a higher fraction of hydrophobic matter, while autochthonous and anthropogenic DOM contain more hydrophilic DOM [26,27].

The hypothesis confirmed in this study is that by examining the characteristics of DOM, it is possible to differentiate between DOM originating from different natural sources (allochthonous and autochthonous), as well as anthropogenic sources.

## 2. Materials and Methods

### 2.1. Study Site

The study was conducted in the upper region of the Otava basin, located in the South Bohemian region of the Czech Republic. This watershed is divided into 14 sub-catchments, with their specific locations depicted in Figure 1 and characteristics described in Table 1. Geological composition of the study area is mainly poorly weatherable metamorphic igneous silicate rock, such as gneiss, paragneiss, and amphibolite. The various sub-catchments exhibit a wide range of characteristics, spanning from lowland areas starting at 360 m a.s.l. to mountains reaching heights of up to 1370 m a.s.l. The lowland regions are predominantly agricultural land with numerous fishponds and scattered small villages. In contrast, the mountain region has dense Norway spruce forests [28]. The climate in this area falls between a maritime and a continental climate, exhibiting transitional characteristics.

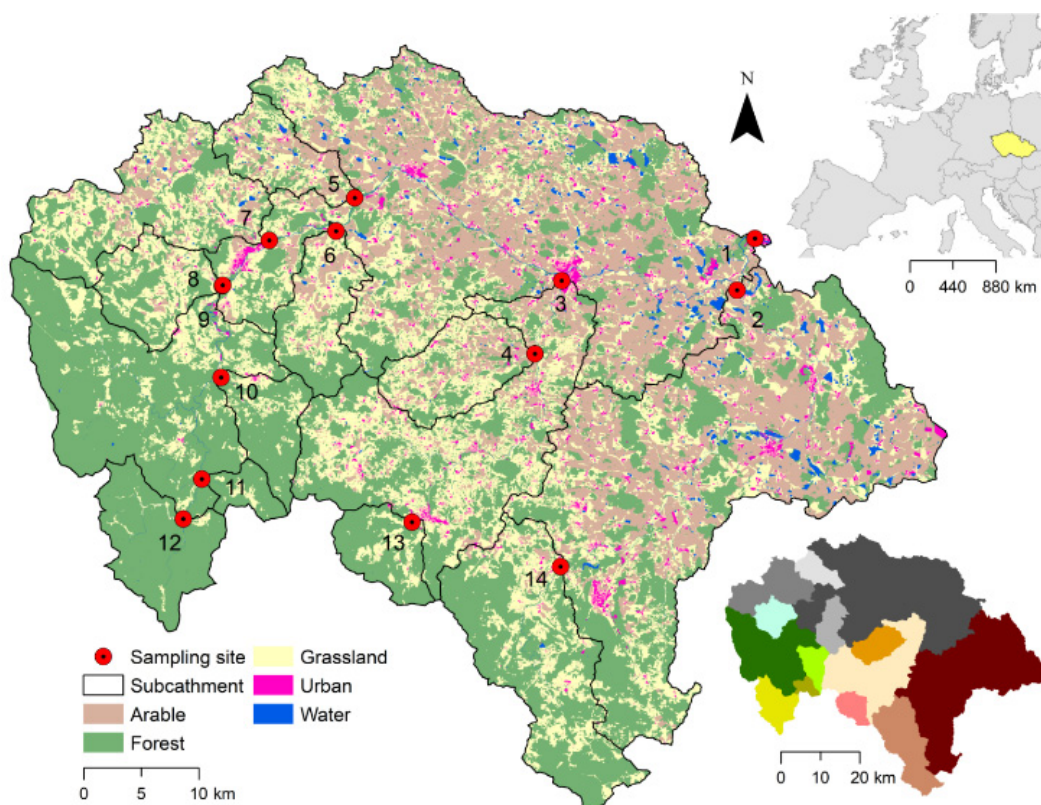


**Figure 1.** Map of the study area in the South Bohemian region of the Czech Republic (**top right**). The studied part of the Otava catchments is divided into 14 sub-catchments (**bottom right**). Sampling sites and land use are shown in the left figure.

**Table 1.** Geographical characteristics of sampling sites and their catchment areas on the river network in the Otava basin. The identification numbers of the sites correspond to Figure 1 for reference.

Site #	1	2	3	4	5	6	7	8	9	10	11	12	13	14
Name	Otava Písek	Blanice Putim	Volyňka Strakonice	Peklov Neměčice	Černíčský Potok Bojanovice	Nezdický Potok Žichovice	Ostružná Sušice	Volšovka Červené Dvorce	Otava nad Volšovkou	Losenice Rejšejn	Hamerický Potok Antýgl	Výdra Modrava	Volyňka Vimperk	Blanice Pode-dvory
Location ( $\frac{N}{E}$ )	49.3083 14.1250	49.2663 14.1127	49.2541 13.9032	49.1947 13.8839	49.2948 13.6435	49.2670 13.6273	49.2521 13.5499	49.2120 13.5026	49.2115 13.5022	49.1405 13.5170	49.0597 13.5120	49.0267 13.4974	49.0506 13.7676	49.0328 13.9504
Altitude m a.s.l.	360	364	400	428	429	435	452	482	465	558	900	980	710	545
Catchment area km <sup>2</sup>	2885	860	427	80.3	61.5	75.8	172	74.4	456	53.7	20.7	89.7	48.4	210
	Land use, %:													
Forest	43.2	40.92	41.5	28.0	27.1	41.1	39.8	50.9	82.1	78.2	86.9	96.2	78.1	64.5
Arable	24.2	28.6	15.1	25.3	30.3	15.3	15.0	4.93	0.36	0.14	0	0.05	0.39	3.07
Grassland <sup>1</sup>	29.1	26.4	40.5	44.2	38.8	41.5	42.7	42.6	16.7	20.8	13.0	3.49	21.1	31.6
Urban	2.23	2.43	2.58	2.19	2.10	1.58	1.73	1.44	0.45	0.75	0.07	0.03	0.34	0.62
Water <sup>2</sup>	1.32	1.6	0.3	0.29	1.69	0.56	0.73	0.13	0.38	0.08	0.09	0.23	0.07	0.23
Population density, person km <sup>-2</sup>	50.0	48.4	57.3	32.0	29.0	22.8	27.3	59.8	9.5	30.7	3.2	0.64	4.2	11.4

Notes: <sup>1</sup> Grassland category includes parks and orchards, <sup>2</sup> Referred to as fishponds in this study.

Monthly samples from these sites were collected over 20 years from 2000 to 2020. Starting in 2021, as part of the DWARF project (Drinking WATER Readiness for the Future, see acknowledgement), this monitoring was continued on a quarterly basis. As an extension of this study, a set of 16 water samples were collected in 2023 from a watercourse that was significantly impacted by fishponds near sample site 3 Volyňka—Strakonice. This watercourse forms a cascade of fishponds, covering approximately 3.9% of the total catchment area.

## 2.2. Trends in Governing Pressures

Based on data from the stations in Strakonice (49.2534 N, 13.9156 E; altitude 404 m a.s.l.) and Churáňov (49.0681 N, 13.6150 E; altitude 1122 m a.s.l.), operated by the Czech Hydrometeorological Institute (<https://www.chmi.cz> (accessed on 2 June 2023)), the annual mean temperature has risen from 5.8 in 1980 to 8.3 °C in 2022, while annual precipitation has increased from 699 to 790 mm. Moreover, the frequency of prolonged droughts and intense rainfall episodes have increased. Despite the changes in climate, the amount of runoff in the Otava river at the main outlet at Písek, with an average of 23.5 m<sup>3</sup> s<sup>-1</sup>, has not shown a significant long-term change. The region has suffered severely due to acidic deposition, particularly in the mountain areas, which have been nitrogen-saturated since the 1960s [29]. Sulphur deposition decreased from 6 g m<sup>-2</sup> in 1985 to 1 g m<sup>-2</sup> by the turn of the century and has gradually declined further to slightly above 0.3 g m<sup>-2</sup>. Both oxidized and reduced nitrogen deposition have decreased from 1.2 to 1.4 g m<sup>-2</sup> in the 1980s to below 0.8 g m<sup>-2</sup> in 2000, stabilizing at around 0.6 g m<sup>-2</sup> over the past two decades. In the administrative region of South Bohemia, to which the Otava basin belongs, the application of fertilization to agricultural land in 2020 was 130, 17, 42, and 73 kg ha<sup>-1</sup> for N, P, K, and Ca, of which 30%, 60%, 75%, and 5%, were added in the form of manure and organic fertilizers, respectively, according to data from the Czech Statistical Office (CZSO) (<https://www.czso.cz> (accessed on 2 June 2023)). During the past 20 years, the



total doses of fertilizers have remained stable, though the proportion of manure has slightly (up to 10%) decreased. Based on summer Normalized Difference Vegetation Index (NDVI) data, Carlson [30] found an increase in biomass across all sub-catchments from 2000 to 2010. Between 2010 and 2020, biomass in the lowlands stabilized or slightly declined, while in the forested mountains, the increase continued, resulting in a total biomass increase of 12% to 17% since 2000. Remarkably, this increase in forest biomass occurred despite a severe bark beetle attack, which caused significant damage to large forested areas [31].

### 2.3. Land Use and Other Catchment Characteristics

Land cover characteristics of the studied catchments were determined using the GIS databases of the Czech Republic (topological-vector database ZABAGED, <https://www.cuzk.cz/> (accessed on 7 June 2023)); public land registry LPIS, (<https://eagri.cz/public/app/lpisext/lpis/verejny2/plpis/> (accessed on 7 June 2023)), and LANDSAT 7 ETM+ satellite images (on the territory of Germany). These land cover data reflect the situation in 2009, though no significant changes have occurred since then. According to census of population, houses, and apartments, provided by the Czech Statistical Office (CZSO), the total population of the basin, which amounted to 140.2 thousand people, remained relatively stable from 2001 to 2020, with a minor decrease of 0.3%.

### 2.4. Biochemical Analysis

This study assesses a comprehensive set of water chemistry data in the Otava river watershed, divided into 14 sub-catchments, covering the period from 2000 to 2022 (Appendix B, Table A3). The data used in this analysis consist of historical monthly records from 2000 to 2020, sourced from the Vltava Basin Authority and Čevak Inc. Additionally, quarterly data from 2021 to 2022, generated by the ongoing DWARF project, are included. The water samples are analyzed for pH, alkalinity, suspended solids (SS), biological oxygen demand (BOD<sub>5</sub>), chemical oxygen demand (COD<sub>Mn</sub> and COD<sub>Cr</sub>), total and/or dissolved organic carbon (TOC, DOC), UV absorbency (Abs. @UV<sub>λ254</sub>), total nitrogen (TOT-N), total phosphorous (TOT-P), chlorophyll A (Chl-a), major cations (Ca<sup>2+</sup>, Mg<sup>2+</sup>, Na<sup>+</sup>, K<sup>+</sup>), major anions (SO<sub>4</sub><sup>2-</sup>, NO<sub>3</sub><sup>-</sup>, Cl<sup>-</sup>), phosphate (PO<sub>4</sub><sup>3-</sup>), and ammonium (NH<sub>4</sub><sup>+</sup>) (Appendix B, Table A3). It is important to note that the monitored parameters varied between sites and over the years. The analytical methods employed by the Vltava Basin Authority for the historic data can be found in Appendix A (Table A1). The DWARF samples underwent pre-filtration in the field using a 200 μm sieve to remove coarse particles. Subsequently, the samples were stored in the dark at 4 °C until analysis within two days. In the laboratory, membrane filters (0.45 μm) were used for ion analysis, while glass-fiber filters (0.4 μm) were used for other analyses. Detailed information regarding the analytical methods employed for the DWARF samples can be found in Appendix A (Table A2).

To investigate the fluorescence characteristics of the DOM, fluorescence excitation-emission intensity (Ex I–Em I) spectra (EEM) were determined for the four seasons in 2021 ( $n = 56$ ) and 2022 ( $n = 56$ ), and the winter season in 2023 ( $n = 14$ ). This analysis was conducted using a Duetta spectrofluorometer (Horiba, France), with an excitation range of 250–550 nm (at 5 nm intervals) and an emission range measured from 280 to 800 nm. Absorbance measurements for inner filter effect correction were simultaneously performed by the instrument. All EEMs were blank-subtracted using the EEM of Milli-Q water obtained on the same day. Moreover, DOM in half of the water samples from 2021 and 2022 ( $n = 56$ ) were fractionated using the method described by Chow et al. [32] into four DOM fractions: Very Hydrophobic Acids (VHA, adsorbed by DAX-8), Slightly Hydrophobic Acids (SHA, adsorbed by XAD-4), Charged Hydrophilic Acids (CHA, adsorbed by IRA-958), and Neutral Hydrophilic Matter (NEU), which was not adsorbed on any of the ion exchange resins.

### 2.5. Derived Parameters and Statistical Analysis

DOM characteristics were determined based on spectroscopic indexes and fractionation (Table A4). The sUV<sub>a</sub> was calculated by normalizing the UV<sub>λ254</sub> value to the DOC concentration. Several indices were determined based on the EEM matrix samples in 2021 and 2022. These include the degree of humification ( $HIX = \frac{\sum I_{Em430-480nm}}{\sum I_{Em300-345nm}} (\lambda_{Ex254nm})$ ) [33], the biological index ( $BIX = \frac{I_{Em380}}{I_{Em430}} (\lambda_{Ex310nm})$ ) [23,34], the fluorescence index ( $FI = \frac{I_{Em470nm}}{I_{Em520nm}} (\lambda_{Ex370nm})$ ) [22,25,35,36], and the spectral ratio ( $SR = \frac{I_{Em\ Slope_{275-295nm}}}{I_{Em\ Slope_{350-400nm}}}$ ) [37]. These indices were derived using the stardom package [38] in the R programming environment [39].

Further, the fluorescence EEM signals were decomposed by the PARAFAC analysis (see Appendix C). This analysis was also computed using the staRdom package in the R programming environment, following the principles outlined by Murphy et al. [24] and Stedmon and Bro [40]. The fluorescence intensities were expressed in Raman units, and various pre-processing steps were applied, including scattering removal, interpolation, data normalization, and the constraint of nonnegativity. No outliers were identified.

Three PARAFAC components were identified that collectively provide a robust description of DOM fluorescence within the dataset, accounting for 98.6% of the total variance in the EEM data matrix. The maximum (and lower) fluorescence intensities were for the three components found at the following excitation and emission wavelengths (nm): component 1 (C1) had the highest fluorescence intensity at  $\lambda_{excitation}/\lambda_{emission}$  265 (365)/487; component 2 (C2) exhibited maximum intensity at  $\lambda_{excitation}/\lambda_{emission}$  250 (305)/413; while component 3 (C3) had a maximum intensity at  $\lambda_{excitation}/\lambda_{emission}$  280/336. The characteristics of the underlying fluorophores were found from matches (Tucker's congruence coefficient (TCC) > 0.95) with the literature in the OpenFluor database [24]: i.e., (C1) high molecular weight humic DOM of allochthonous origin and associated with a high degree of aromaticity [41–43]; (C2) medium molecular weight fulvic DOM, likely derived from microbial reprocessing in the water [41,44]; and (C3) protein-like material. The latter is customarily linked to anthropogenic sources [45,46]. The relative fluorescence intensity of each component (%C<sub>i</sub>), expressed as a percentage of the sum of the three components, was used for further analyses. Model validation procedures, including visual evaluation of spectral loadings, leverages, sample residuals, and split-half analysis (TCC > 0.996), were performed. Additional details regarding the model, validation, and literature matches can be found in Appendix C. All statistical analysis (i.e., correlation, cluster and PCA) were performed in MiniTab Statistical software (Version 21.1.1).

## 3. Results and Discussions

### 3.1. Land Use as a Governing Factor on Spatial Differences in Water Chemistry

The lowland rivers in the Otava basin exhibit higher ionic strength and elevated levels of DOC, COD<sub>Mn</sub>, nutrients (TOT-P, TOT-N, K<sup>+</sup>), and Chl-a. In contrast, streams draining the upland regions have more diluted waters with lower levels of DOC and no Chl-a. Comparing the average physicochemical characteristics of water at each of the 14 sites to the land-use composition of their respective catchments reveals the strong influence of land use on water quality (Figure 2). The percentage of arable land in the catchments governs the levels of TOT-P and K<sup>+</sup> in the waters (Figure 2A). This relationship is likely attributed to increased erosion in ploughed fields and the use of fertilizers in agricultural practices. BOD<sub>5</sub> and SS are mainly influenced by the water coverage in the lowland region (Figure 2B). Despite the relatively small land cover percentage of surface water, its impact in this region is substantial due to the prevalence of fish farming. Consequently, these surface waters, referred to as fishponds, play a significant role in both water and DOM quality. The levels of TOT-P, K<sup>+</sup>, and NO<sub>3</sub><sup>-</sup> are also influenced by the limited extent of urban coverage (Figure 2C), likely due to the discharge of untreated and incompletely treated sewage. On the contrary, the percentage of forest cover exhibits a negative relationship with alkalinity, TOT-N, K<sup>+</sup>, and Cl<sup>-</sup> levels in the drainage waters (Figure 2D). Forests are typically grown

on acidic soils derived from poorly weatherable minerals, rendering relatively acidic runoff characterized by low ion concentrations. The average sUVA values for each catchment are primarily governed by the percentage of forest cover (Figure 3), explaining 70.6% of the variation. Conversely, the percentage of arable land shows a negative correlation with sUVA ( $R^2 = 0.491$ ). sUVA values above 0.033 are only observed in sites with more than 50% forested land (Figure 3). This reflects that forests serve as a major source of allochthonous DOM with high specific absorbency ratios. In contrast, watersheds with arable land primarily receive autochthonous and anthropogenic DOM with lower sUVA values.

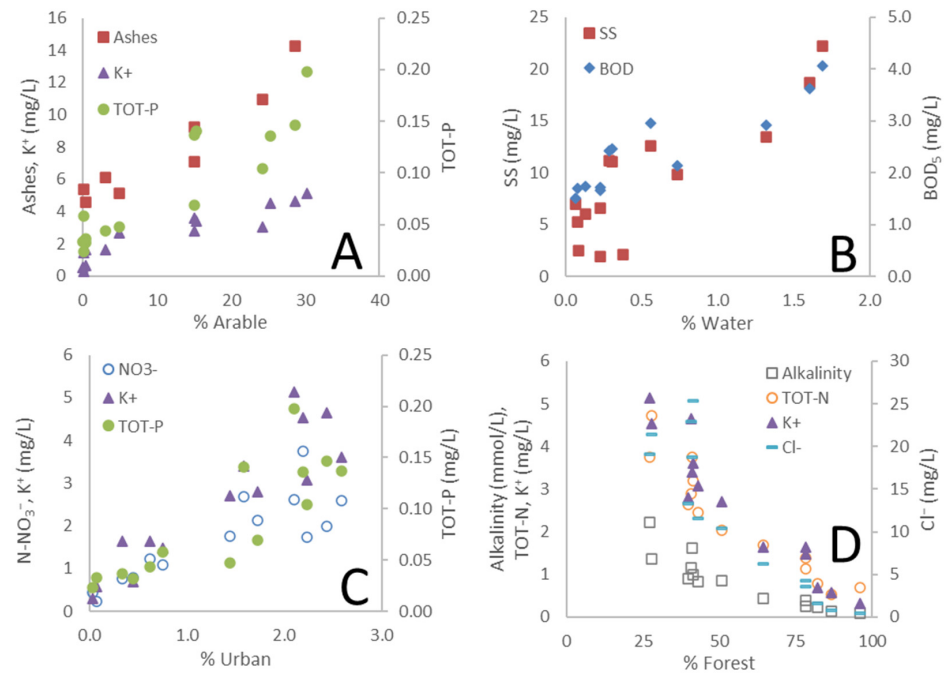


**Figure 2.** Relationship between mean concentration (all historic data) of related chemical parameters in streams and the percentage of different land use (i.e., (A) arable land, (B) water surface, i.e., fishponds, (C) urban area, and (D) forested area) in the 14 sub-catchments draining into the streams.

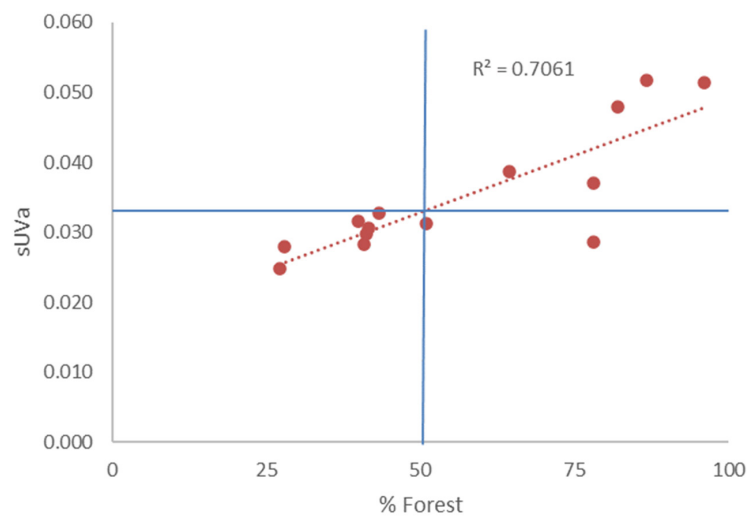


**Figure 3.** Correlation between site average sUVA ( $\text{cm}^{-1}/\text{mg C/L}$ ) in the DWARF data (2021 and 2022) vs. percent forest in the watersheds drained by the stream. Blue horizontal line denotes threshold values for significant content of autochthonous and anthropogenic DOM (below) relative to allochthonous DOM (above). Blue vertical line denotes limit value for insignificant content of autochthonous and anthropogenic DOM.

### 3.2. Governing Factors on DOM

Over the past 20 years, the concentration of DOC and  $\text{COD}_{\text{Mn}}$  in the main outlet of the Otava river (Site 1, Figure 1) has increased by 14% and 30%, respectively. Moreover, the runoff from areas predominantly used for agriculture has shown a significant increase in  $\text{BOD}_5$  (e.g., 40% increase at Site 5 Černíčský potok—Bojanovice). In contrast, sub-catchments dominated by forests (e.g., Site 13 Volyňka—Vimperk) exhibited no significant trends in DOC nor  $\text{COD}_{\text{Mn}}$ . This suggests that the rise in DOC and  $\text{COD}_{\text{Mn}}$  at the main outlet of the Otava river is primarily attributed to increased flux of DOM from lowland sites. Conversely, data from forested ICP-water monitoring sites (data—ICP Waters (icp-waters.no)), located further north in the Šumava mountains, generally indicate slight increasing trends in DOC since 1993.

There is a strong correlation between TOC and DOC values ( $R^2 = 0.976$ ). However, a ratio of 0.80 in the linear regression equation indicates that 20% of TOC exists in the form of particulate organic matter (POC). This POC includes algae, which is measured as Chl-a. Elevated levels of SS commonly serve as an indicator of local anthropogenic sources of organic matter, such as sewage and overland flow flushing manure from fertilized soils, which can also lead to algae blooms (high Chl-a) due to eutrophication. SS is thus found to be positively correlated with biochemical oxygen demand ( $\text{BOD}_5$ ) ( $R^2 = 0.933$ ).

$\text{UV}_{\lambda 254}$  is strongly correlated to DOC ( $R^2 = 0.908$ ). Despite this strong correlation,  $\text{sUVA}$  values are a useful indicator to distinguish allochthonous DOM from autochthonous and anthropogenic DOM.  $\text{sUVA}$  is negatively correlated with the  $\text{BOD}_5/\text{COD}_{\text{Mn}}$  ratio, reaching a plateau at  $\text{sUVA}$  values below 0.033 and  $\text{BOD}_5/\text{COD}_{\text{Mn}}$  ratios above 0.5 (Figure 4). This suggests that when more than 50% of the  $\text{COD}_{\text{Mn}}$  is biodegradable,  $\text{sUVA}$  values are below 0.033, indicating a significant content of autochthonous or anthropogenic DOM. The threshold value of 0.033 is supported by an assessment of more pristine Norwegian freshwaters [19]. However, Figure 4 also demonstrates that  $\text{sUVA}$  values below 0.033 can be found in samples with  $\text{BOD}_5/\text{COD}_{\text{Mn}}$  ratios below 0.5, implying less anthropogenic influence. Low  $\text{sUVA}$  values are thus only an indication that there may be some anthropogenic influence. Furthermore, average  $\text{sUVA}$  values for each site are negatively co-correlated with average pH ( $R^2 = 0.648$ ), with higher  $\text{sUVA}$  values observed in low-pH dystrophic waters. This reflects that stream waters with high  $\text{sUVA}$  values are dominated by allochthonous DOM from the acid and forested headwater catchments, while those with low  $\text{sUVA}$  values have more autochthonous or anthropogenic DOM from the more buffered lowland agricultural region. This was also found among two pristine Nordic sites (i.e., Svartberget and Hietajärvi) that were not strongly affected by acid rain [26].

The biological index (BIX) and fluorescence index (FI), which serve as proxies for autochthonous and microbially derived DOM, respectively, are positively correlated ( $R^2 = 0.693$ ). Average BIX values for each site (Table A4) tend to be lower in runoff from forested and wetland-dominated catchments (Figure 5A) and higher in watersheds dominated by arable land, grassland, and urban areas (Table 1). BIX, on the other hand, is negatively correlated with the percentage of forest cover (Figure 5B). These findings align with Huguet et al. [23] that concluded that DOM with low BIX values has a low autochthonous component, while high values indicate a strong autochthonous component. Furthermore, BIX demonstrates a strong positive correlation with certain chemical parameters associated with anthropogenic loading, such as alkalinity ( $R^2 = 0.678$ ) and  $\text{SO}_4^{2-}$  ( $R^2 = 0.783$ ). The humification index (HIX) distinguishes between DOM with strong humic traits, originating mainly from allochthonous sources, and the DOM with weak humic character, derived mainly from autochthonous source. Surprisingly, the site average HIX was not found to correlate with any specific land use, nor with any other DOM characteristics or inorganic parameters ( $R^2 < 0.3$ ). This is partly explained in Section 3.4 by a strong influence of fishponds on the HIX and suggests that the HIX loosely responds to differences in humification of DOM between forested sites and fishponds (with high humification and  $\text{sUVA}$ ) relative to grassland and agricultural sites (low humification and high calcium concentration). Fortunately,  $\text{sUVA}$ , which is a more readily available parameter, shows a



strong correlation with BIX ( $R^2 = 0.940$ ) and FI ( $R^2 = 0.921$ ), allowing sUVa to be employed as a simple proxy for assessing the relative amounts of allochthonous vs. autochthonous or anthropogenic DOM. The allochthonous humic matter is characterized by relatively high molecular weight aromatic compounds, while autochthonous fulvic moieties of the DOM are more low molecular weight and aliphatic (Perdue, 2009). The spectral ratio (SR), which is inversely related to the molecular size, is thus negatively correlated ( $R^2 = 0.403$ ) to sUVa, a proxy for aromaticity. At sUVa values below 0.033, the link between SR and sUVa is weak (Figure 6), due to the mix with anthropogenic DOM, having  $BOD_5/COD_{Mn}$  ratios above 0.5 [19], i.e., DOM from fishponds is characterized by having high SR and sUVa, expressing low molecular weight and high aromaticity (see Section 3.3). The C1 component, ascertained as high molecular weight humic DOM and associated with a high degree of aromaticity, was, as could be expected, negatively correlated to SR ( $R^2 = 0.451$ ) and positively correlated to sUVa ( $R^2 = 0.744$ ). Moreover, C1 was strongly negatively correlated to BIX ( $R^2 = 0.924$ ), reflecting the low autochthonous contribution in samples with a high C1 component. Site-averaged C1 was thus strongest correlated to the relative forest cover ( $R^2 = 0.915$ ). The fulvic DOM comprising the C2 component was found to be strongest correlated to FI ( $R^2 = 0.851$ ), reflecting microbially derived autochthonous DOM. Site average values for this component were thus negatively correlated to the relative forest cover ( $R^2 = 0.874$ ). Surprisingly, site average values of the protein-like material (C3) were weakly correlated to water (fishpond) cover; instead, they were strongly correlated to the relative proportion of urban development ( $R^2 = 0.821$ ), possibly reflecting the influence of sewage.

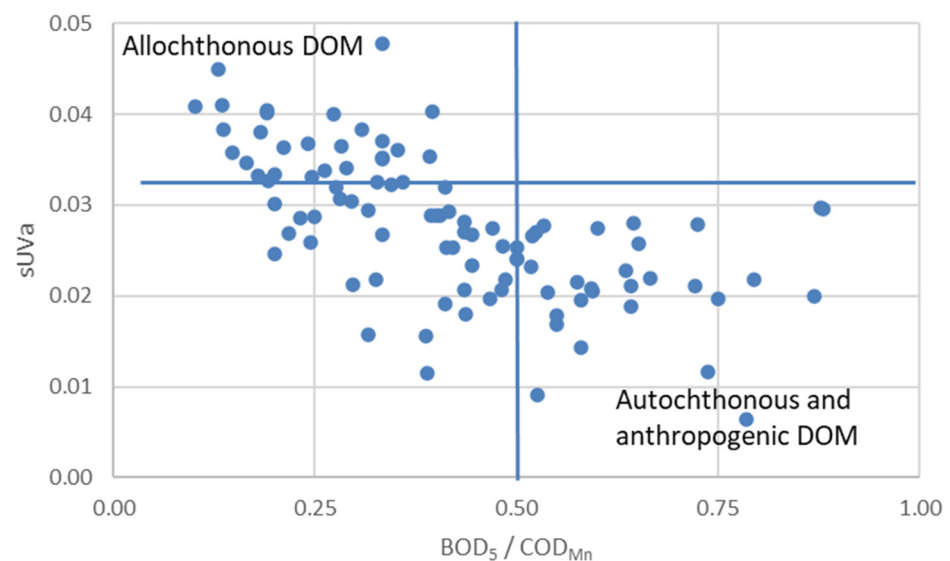


**Figure 4.** Correlation between sUVa ( $\text{cm}^{-1}/\text{mg C/L}$ ) and the ratio of  $BOD_5$  over  $COD_{Mn}$ , both reflecting the content of autochthonous and anthropogenic relative to allochthonous DOM in the water. The data are from Losenice (Site 10) sampled between 2000 and 2020. Blue horizontal and vertical lines denote threshold values for significant content of autochthonous and anthropogenic DOM relative to allochthonous DOM.

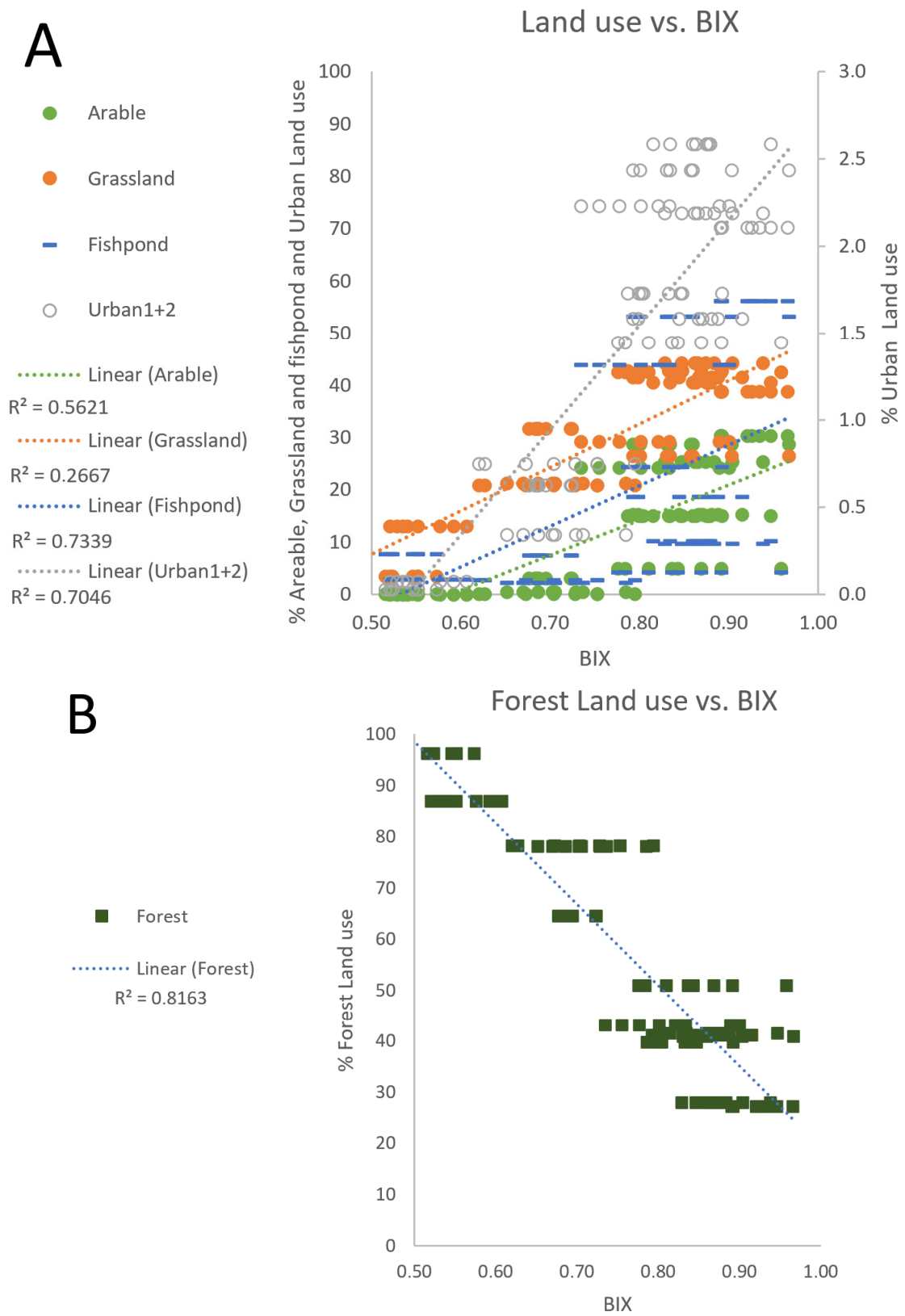


**Figure 5.** Relationship between different land uses and biological index (BIX) reflecting the contribution of autochthonous (and anthropogenic) relative to allochthonous DOM sources: (A) arable, grassland, parks and orchards, fishponds (i.e., water), and urban areas; and (B) forest. Data are from seasonal samples collected in 2021 and 2022.

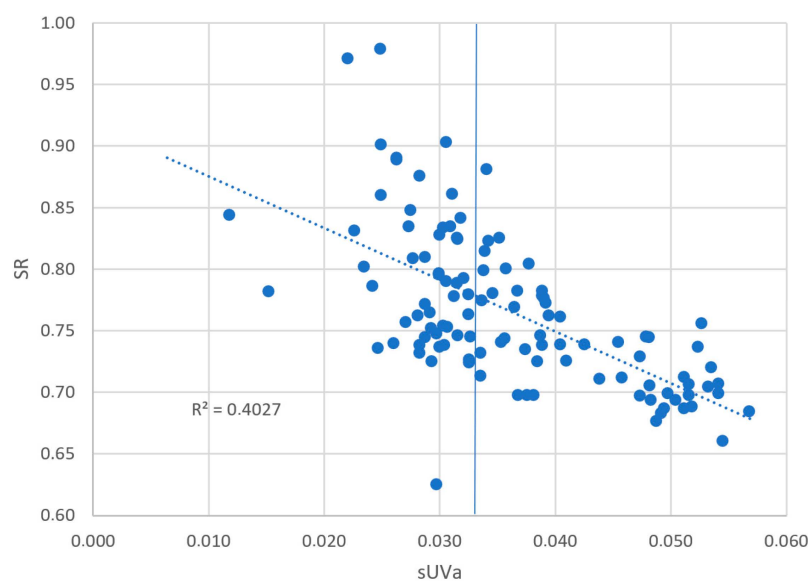


**Figure 6.** Relationship between the spectral ratio (SR) and specific UV adsorption (sUVa) reflecting the link between size and aromaticity in the allochthonous and autochthonous sources of DOM at sUVa values above 0.033. The correlation is weak in samples with sUVa below 0.033 due to the influence of anthropogenic DOM. Data are from seasonal samples collected in 2021 and 2022.

The relative proportions of hydrophilic moieties of the DOM, represented by the hydrophilic index (HPI) as the sum of the percentage charged hydrophilic acids (CHA) and neutrals (NEU), were significantly higher in our studied waters (HPI = 23.7%) (Table A4) compared to 10 pristine raw water sources used for drinking water production in the Nordic countries and Scotland (15.4%) [47]. This disparity is primarily attributed to the substantial human influence in the watersheds, leading to increased levels of autochthonous and anthropogenic HPI DOM in our samples. Notably, the proportion of the NEU fraction was more than twice the size, while the slightly hydrophobic acids (SHA) accounted for less than half of what was found in the more pristine sites. On average, sites 5 to 8 (Figure 1, Table 1) had the lowest relative proportion of very hydrophobic acids (VHA) in the DOM, constituting only 59% of the DOM, primarily due to a more significant contribution by SHA (13%). These sites are small sub-catchments in the upper lowland region of the Otava river, characterized by a mixture of different land use types. Notably, seasonal fluctuations were observed in SHA, particularly at these four sites, with negligible amounts detected in the fall samples, possibly associated with specific land-use practices. The average proportion of VHA was strongly correlated with the site's average sUVa (Table 2), with the highest fraction of VHA found at sites 11 and 12 (Table A4) that have extensive forest cover (Table 1), though the overall correlation to forest cover was not significant ( $p < 0.001$ ). Still, this reflects the stronger influence of allochthonous hydrophobic humic DOM from the forests at these sites. Furthermore, HPI moieties were correlated with the coverage of fishponds and BOD<sub>5</sub> (Table 2). Interestingly, the relative respiration rate of the DOM (Rel. RR, unpublished data), serving as a proxy for biodegradability [48], also exhibited a strong negative correlation with the proportion of VHA (Table 2). This adheres to the fact that the high molecular and aromatic VHA fraction has a lower biodegradability than other DOM moieties. Additionally, the relative amounts of charged hydrophilic acids (CHA) exhibited significant correlations with urban land coverage, as well as potassium (K<sup>+</sup>) and nitrate (NO<sub>3</sub><sup>-</sup>) concentrations, along with BIX, FI, and HIX values (Table 2). This suggests that CHA, along with the C3, could potentially serve as tracers for sewage, enabling the differentiation of urban sewage-derived DOM from allochthonous DOM found in eutrophic lakes and fishponds.

**Table 2.** Coefficient of determination for significant ( $p < 0.001$ ) correlations between DOM fractions and explanatory factors. Data are from four sets of seasonal samples ( $n = 56$ ) collected in 2021 and 2022.

%DOM Fractions	vs.	$R^2$
HPI	Fishponds	0.712
	BOD <sub>5</sub>	0.810
	Rel. RR	0.691
VHA	sUVa	0.669
CHA	Urban	0.689
	COD <sub>Mn</sub>	0.729
	K <sup>+</sup>	0.676
	NO <sub>3</sub> <sup>-</sup>	0.729
	BIX	0.757
	FI	0.805
	HIX	0.704

### 3.3. Multivariate Statistics

A cluster analysis incorporating water chemistry, sUVa and catchment land-use, along with the parallel factor analysis (PARAFAC) components on the quarterly data from 2020 and 2021, provides confirmation regarding associations with the components C1 and C2 (Figure 7) described above. The humic DOM component (C1) is primarily observed in runoff from acidic forested sites and peatlands, characterized by allochthonous DOM with high specific UV absorbance (sUVa). A cluster with DOC and H<sup>+</sup> is closely linked to this mountain forest cluster. In a study of almost five thousand Fennoscandian lakes, Crapart et al. [49] also found that forest cover is a strong spatial predictor for DOC. This connection underscores the significance of forested headwaters in contributing to the variation in DOC levels. The fulvic DOM component (C2) is linked to runoff originating from lowland grassland areas, including parks and orchards, which exhibit high nitrogen content. These areas tend to have more autochthonous DOM with a high biological index (BIX). The water chemistry from grasslands is closely associated with a subcluster formed by samples in the lowland region with arable and urban land cover, generating runoff with high alkalinity, ionic strength, and potassium. This is likely due to the liming of agricultural land. On the other hand, protein-like material (C3) in the PCA is closer associated to catchments influenced by fishponds than to urban land. A cluster analysis also comprising the DOM fractions, on only half of the quarterly data (Appendix D, Figure A4), placed the VHA in the cluster with humic DOM, NEU along with fulvic DOM, and CHA and SHA together with protein-like material from the fishponds.

In summary, the cluster analysis with PARAFAC components and DOM fractions confirm the distinct patterns of DOM composition across different land-use types, indicating the dominance of very hydrophobic allochthonous humic DOM in mountain forested areas, neutral hydrophilic autochthonous fulvic DOM in the lowland grassland regions, as well as in arable environments. The slightly hydrophobic acids (SHAs) or charged hydrophilic (CHA) protein-like material is closer associated to runoff from fishponds than from urban environments, as found in Section 3.1.

A Principal Component Analysis (PCA), also conducted on the quarterly dataset (Figure 8), gave a first Principal Component (PC1) representing an allochthonous–autochthonous gradient that accounts for 71.8% of the data variation. It effectively separates the allochthonous humic DOM from the autochthonous fulvic DOM and the anthropogenic protein-like material. The second Principal Component (PC2), explaining an additional 9.0% of the variation, represents a DOM gradient. It does not deconvolute the sources of autochthonous fulvic DOM from the anthropogenic protein-like material. When plotted on the PC1 vs. PC2 plane, the four clusters identified in the cluster analysis (Figure 7) can be recognized within the PCA. The third Principal Component (PC3), explaining an additional 5.5% of the variation in the dataset, separates the clusters with fulvic DOM in regions with



grassland and urban development from the cluster with protein-like material (Appendix D, Figure A5) from fishponds.

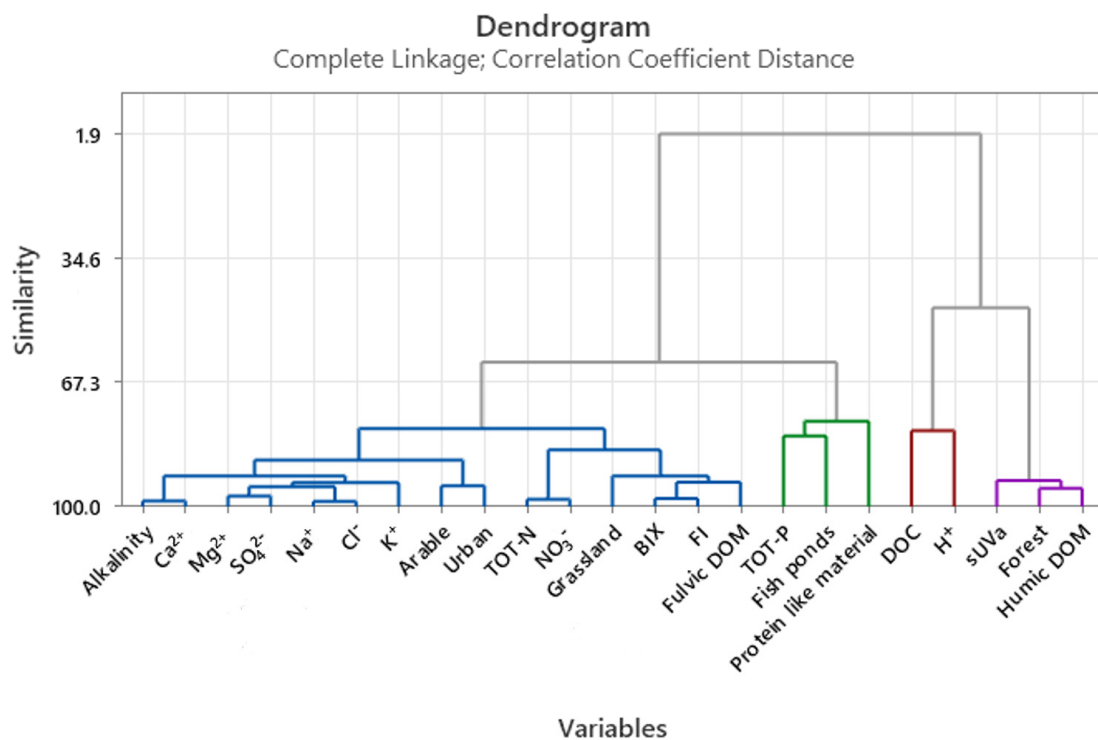


**Figure 7.** Cluster analysis of the water chemistry, sUVa, and catchment land use, along with the three PARAFAC component groups (Humic DOM (C1), Fulvic DOM (C2) and Protein like DOM (C3)) on the quarterly data from 2021 to 2022.

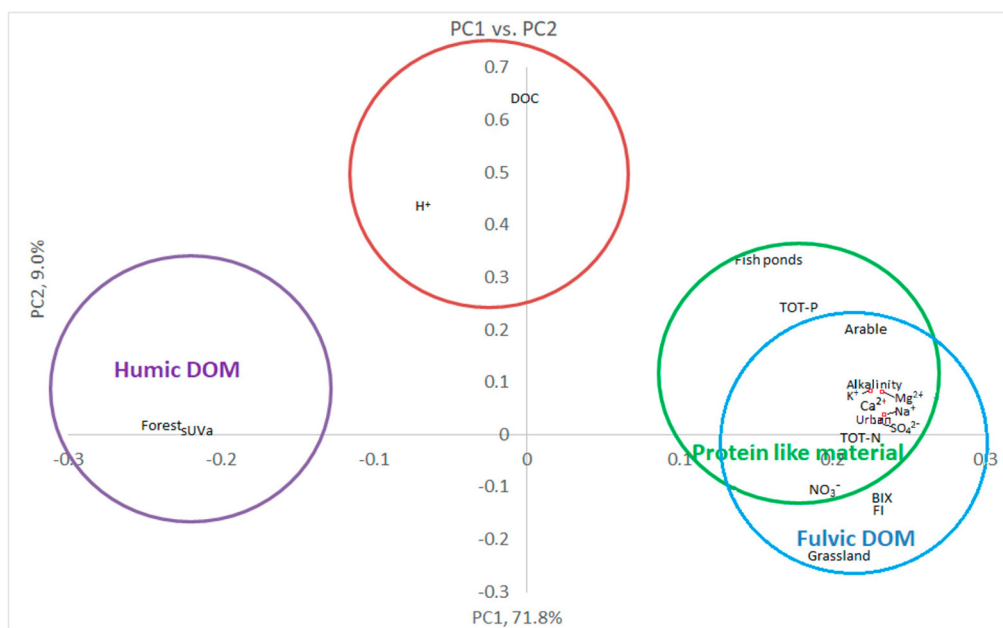


**Figure 8.** The 1st and 2nd Principal Component (PC) from a Principal Component Analysis of the three PARAFAC component groups, catchment characteristics, and water chemistry.

In summary, the PCA results demonstrate the presence of distinct gradients in the data, with PC1 representing the distinction between allochthonous and autochthonous DOM and PC3 capturing the differentiation between autochthonous and anthropogenic DOM from sewage on the one side and anthropogenic DOM from fishponds on the other. The PCA plot confirms the clustering patterns observed in the cluster analysis and highlights the role of fishponds in driving an anthropogenic component of autochthonous DOM at the studied sites.

#### 3.4. Fishpond Study

Correlation and multivariate analysis in Sections 3.2 and 3.3 differ in their assessment of sources for the protein-like components (C3). In order to address this, water samples were collected from a watercourse heavily influenced by fishponds. These waters exhibited average concentrations of DOC (10.4 mg C/L), SS (22.6 mg/L), and TOT-P (0.4 mg/L) that were 1.7, 2.5, and 4.7 times higher than the average for the 14 sites, respectively (Appendix B, Table A3). Also, the DOM in these waters displayed distinct features, including high values for BIX (1.0), FI (1.4), sUVa (0.056), and SR (1.0), relative to the values for 14 studied sites (Appendix B, Table A4). The elevated BIX and FI values, reflecting strong recent autochthonous contribution of autochthonous DOM derived from microbial activity, suggest that the DOM in these eutrophic ponds is predominantly derived from autochthonous sources and influenced by microbial activity, similar to the characteristics of autochthonous fulvic acids. On the other hand, it was noteworthy that the sUVa values were high, indicating that the DOM in the fishponds exhibits significant aromatic characteristics. The sUVa data are supported by a significant correlation with the humification index (HIX) ( $R^2 = 0.689$ ). This heightened aromaticity can serve as a useful distinguishing factor, allowing the differentiation of DOM originating from fishponds from other sources of autochthonous and anthropogenic fulvic DOM, which typically exhibit lower levels of aromaticity.

In summary, the water samples collected from the streams affected by fishponds exhibited specific chemical and DOM characteristics, including high SR and sUVa values. These features are indicative of low molecular aromatic DOM. This aromatic nature of DOM originating from the fishponds distinguishes the DOM from fishponds from other autochthonous and anthropogenic sources of fulvic DOM.

#### 4. Conclusions

This study highlights the applicability of using DOM characteristics to deconvolute the sources of dissolved organic matter. In the Otava watercourses, these sources are as follows: (1) allochthonous high molecular weight and aromatic humic DOM originating from mountainous conifer forests and wetlands, (2) autochthonous low molecular weight and aliphatic fulvic DOM derived from algae growth due to eutrophication in the lowlands, and (3) anthropogenic DOM containing protein-like material from sewage and fishponds. The relative proportions of allochthonous DOM can be distinguished from the autochthonous and anthropogenic DOM by examining the biological index (BIX) or simply by assessing the specific UV absorbance (sUVa). Autochthonous fulvic DOM originating from eutrophic waters can be distinguished from anthropogenic DOM originating from sewage and fishponds through the presence of protein-like material (C3) or by the third PC of a PCA. Furthermore, anthropogenic DOM from fishponds can potentially be differentiated from autochthonous and sewage DOM by rather uniquely displaying a high sUVa along with a high Spectral Slope Ratio (SR). Moreover, anthropogenic DOM from fish farms is characterized by higher moieties of charged and slightly hydrophobic acid, while autochthonous DOM and sewage has higher levels of neutral hydrophilic matter.

In summary, DOM characteristics provide valuable tools for differentiating between the various sources of DOM. Allochthonous DOM can likely be distinguished by high sUVa, autochthonous fulvic DOM can be identified by a higher BIX and FI, and anthropogenic DOM from sewage (and fishponds) can be distinguished from autochthonous DOM by a

high content of protein-like matter (C3). Finally, DOM from fishponds differs from sewage by possessing a high sUVa, as well as a higher fraction of charged hydrophilic and slightly hydrophobic organic acids.

**Author Contributions:** Conceptualization, R.D.V., P.P. and J.H.; methodology, P.P., J.H., G.I.O. and B.E.; software, R.D.V. and C.B.G.; formal analysis, R.D.V. and J.H.; investigation, P.P. and J.H.; resources, P.P.; data curation, P.P. and J.H.; writing—original draft preparation, R.D.V.; writing—review and editing, R.D.V., J.H., M.C.P.-M., S.H., G.I.O. and C.B.G.; visualization, R.D.V. and M.C.P.-M.; project administration, P.P.; funding acquisition, P.P. All authors have read and agreed to the published version of the manuscript.

**Funding:** The analysis of water composition was supported and funded by the Czech Science Foundation (project No. P503-22-05421S) and the TAČR KAPPA project Drinking Water Readiness for the Future (DWARF) was funded by the Norway Grants. No. 2020TO01000202.

**Data Availability Statement:** The data used in this analysis consist of historical records from 2000 to 2020, sourced from the Vltava Basin Authority and Čevak Inc. Additionally, quarterly data from 2021 to 2022, generated by the ongoing DWARF project (Drinking Water Readiness for the Future), are included. All data are stored in the databases of the Biology Centre CAS, Institute of Hydrobiology, 370 05 České Budějovice, Czech Republic.

**Conflicts of Interest:** The authors declare no conflict of interest.

## Appendix A

**Table A1.** Physical and chemical parameters and methods of analysis used to characterize water quality in the Otava basin by the Vltava Basin Authorities from 2000 to 2020.

Parameter	Method of Analysis/Instrument	Ref.
pH	Probe YSI 6600 V2-4 (Xylem Inc.)	-
Suspended solids (mg L <sup>-1</sup> )	Gravimetry after drying at 105 °C	[50]
Alkalinity	Titrimetric determination of acid neutralizing capacity to pH 4.5 (ANC <sub>4.5</sub> )	[51]
Biochemical oxygen demand after 5 days (BOD <sub>5</sub> , mg L <sup>-1</sup> )	Electrochemical or optical probe methods	[52]
Chemical oxygen demand by permanganate (COD <sub>Mn</sub> , mg L <sup>-1</sup> )	Titrimetric determination after digestion with permanganate	[53]
Chemical oxygen demand by dichromate method (COD <sub>Cr</sub> , mg L <sup>-1</sup> )	Spectrophotometric test tube method	[54]
UV absorbency (Abs. @UV <sub>λ254</sub> )	Spectrometry (Shimadzu UV-1650 PC)	[55]
TOT-P (mg L <sup>-1</sup> )	Inductive coupled plasma spectrometry (Agilent 8800 ICP-MSQ)	[56]
PO <sub>4</sub> <sup>3-</sup> (mg L <sup>-1</sup> )	Spectrophotometric ammonium molybdate method (Shimadzu UV-1650 PC)	[57]
TOT-N (mg L <sup>-1</sup> )	High-temperature combustion (Multi N/C 2100 analyzer, Analytik Jena AG, Germany) with unfiltered water samples	[58]
N-NH <sub>4</sub> <sup>+</sup> (mg L <sup>-1</sup> )	Spectrophotometry (Shimadzu UV-1650 PC)	[59]
SO <sub>4</sub> <sup>2-</sup> , N-NO <sub>3</sub> <sup>-</sup> , Cl <sup>-</sup> , (mg L <sup>-1</sup> )	Ion chromatography (Dionex ICS-1000)	[60]
Ca <sup>2+</sup> , Mg <sup>2+</sup> , Na <sup>+</sup> , K <sup>+</sup> (mg L <sup>-1</sup> )	Ion chromatography (Dionex ICS-1000)	[61]
Chl-a (μg L <sup>-1</sup> )	Spectrometry (Shimadzu UV-1650 PC)	[62]
TC (mg L <sup>-1</sup> )	High-temperature combustion method (Multi N/C 2100 analyzer, Analytik Jena AG, Germany)	[63]
TIC (mg L <sup>-1</sup> )	Low-temperature acidification method (Multi N/C 2100 analyzer, Analytik Jena AG, Germany)	[63]
TOC (mg L <sup>-1</sup> )	TOC = TC – TIC	[63]
DC (mg L <sup>-1</sup> )	High-temperature combustion method (Multi N/C 2100 analyzer, Analytik Jena AG, Germany)	[63]
DIC (mg L <sup>-1</sup> )	Low temperature acidification method (Multi N/C 2100 analyzer, Analytik Jena AG, Germany)	[63]
DOC (mg L <sup>-1</sup> )	DOC = DC – DIC	[63]

**Table A2.** Physical and chemical parameters and methods of analysis used to characterize water quality in the Otava basin by the DWARF project from 2020 to 2022.

Parameter	Method of Analysis/Instrument	Ref.
pH	TIM865, Radiometer	-
Suspended solids (mg L <sup>-1</sup> )	Gravimetry after drying at 105 °C	[50]
Alkalinity	Titrimetric determination of acid neutralizing capacity according to Gran using TIM865, Radiometer	[51]
UV absorbency (Abs. @UV <sub>λ254</sub> )	Spectrometry (Shimadzu UV-2700)	[55]
TOT-P (mg L <sup>-1</sup> )	Spectrophotometric molybdate method (Kopáček and Hejzlar, 1993)	[57]
PO <sub>4</sub> <sup>3-</sup> (mg L <sup>-1</sup> )	Spectrophotometric ammonium molybdate method (Specord 50, Analytik Jena) Murphy and Riley (1962)	[57]
Tot-N (mg L <sup>-1</sup> )	High-temperature combustion (Shimadzu TOC-L) with unfiltered water samples	[58]
N-NH <sub>4</sub> <sup>+</sup> (mg L <sup>-1</sup> )	Spectrophotometry (Specord 50, Analytik Jena)	[59]
N-NO <sub>3</sub> <sup>-</sup> , Cl <sup>-</sup> , SO <sub>4</sub> <sup>2-</sup> (mg L <sup>-1</sup> )	Ion chromatography (Dionex ICS-5000+)	[60]
Ca <sup>2+</sup> , Mg <sup>2+</sup> , Na <sup>+</sup> , K <sup>+</sup> (mg L <sup>-1</sup> )	Ion chromatography (Dionex IC25)	[61]
TOC (mg L <sup>-1</sup> )	Nonpurgable total organic carbon (Shimadzu TOC-5000A)	[63]
DOC (mg L <sup>-1</sup> )	Nonpurgable dissolved organic carbon (Shimadzu TOC-L)	[63]

## Appendix B

**Table A3.** Average inorganic water chemistry at each site, along with its standard deviation and the amount of data for each parameter and site.

Site #	pH	Alkalinity mmol L <sup>-1</sup>	SS mg L <sup>-1</sup>	TOT-N mg L <sup>-1</sup>	TOT-P mg L <sup>-1</sup>	Ca <sup>2+</sup> mg L <sup>-1</sup>	Mg <sup>2+</sup> mg L <sup>-1</sup>	Na <sup>+</sup> mg L <sup>-1</sup>	K <sup>+</sup> mg L <sup>-1</sup>	SO <sub>4</sub> <sup>2-</sup> mg L <sup>-1</sup>	NO <sub>3</sub> <sup>-</sup> mg L <sup>-1</sup>	Cl <sup>-</sup> mg L <sup>-1</sup>	PO <sub>4</sub> <sup>3-</sup> mg L <sup>-1</sup>	N-NH <sub>4</sub> <sup>+</sup> mg L <sup>-1</sup>
1	7.53	0.83	13.5	2.45	0.10	14.5	5.60	7.51	3.07	22.2	1.73	11.6	0.05	0.09
2	7.45	1.14	18.7	2.89	0.15	24.1	8.83	15.1	4.65	33.3	1.99	22.9	0.05	0.11
3	7.58	0.99	11.1	3.19	0.14	22.5	7.06	14.9	3.61	24.7	2.60	25.4	0.09	0.08
4	7.51	1.36	11.2	4.71	0.14	28.5	9.88	13.6	4.54	35.4	3.74	21.4	0.10	0.09
5	7.80	2.23	22.2	3.75	0.20	40.3	14.2	15.5	5.13	44.8	2.61	19.1	0.09	0.14
6	7.76	1.61	12.6	3.74	0.14	35.3	9.38	11.5	3.41	29.4	2.67	18.7	0.10	0.28
7	7.45	0.89	9.85	2.63	0.07	14.9	6.17	8.72	2.80	21.1	2.14	13.4	0.03	0.06
8	7.53	0.85	5.99	2.04	0.05	18.3	4.59	7.50	2.71	17.4	1.75	10.4	0.02	0.04
9	7.00	0.22	2.10	0.78	0.03	3.80	1.00	2.59	0.69	4.41	0.78	1.64	0.02	0.01
10	7.18	0.39	5.25	1.38	0.06	8.58	2.41	4.30	1.49	11.4	1.08	4.28	0.04	0.04
11	6.57	0.12	2.54	0.52	0.03	1.84	0.53	2.03	0.57	3.05	0.24	0.75	0.02	0.00
12	5.72	0.10	1.92	0.68	0.02	1.47	0.43	1.43	0.31	1.45	0.44	0.41	0.01	0.03
13	7.14	0.26	7.03	1.13	0.04	2.78	1.71	4.38	1.63	12.0	0.76	3.57	0.01	0.02
14	7.45	0.44	6.64	1.68	0.04	6.28	3.99	13.4	1.66	12.4	1.23	6.19	0.02	0.03



Table A3. Cont.

Site	pH	Alkalinity	SS	TOT-N	TOT-P	Ca <sup>2+</sup>	Mg <sup>2+</sup>	Na <sup>+</sup>	K <sup>+</sup>	SO <sub>4</sub> <sup>2-</sup>	NO <sub>3</sub> <sup>-</sup>	Cl <sup>-</sup>	PO <sub>4</sub> <sup>3-</sup>	N-NH <sub>4</sub> <sup>+</sup>
#		mmol L <sup>-1</sup>	mg L <sup>-1</sup>	mg L <sup>-1</sup>	mg L <sup>-1</sup>	mg L <sup>-1</sup>	mg L <sup>-1</sup>	mg L <sup>-1</sup>	mg L <sup>-1</sup>	mg L <sup>-1</sup>	mg L <sup>-1</sup>	mg L <sup>-1</sup>	mg L <sup>-1</sup>	mg L <sup>-1</sup>
1	0.02	0.23	24.2	1.04	0.05	5.37	2.09	2.36	1.01	6.98	0.92	4.03	0.03	0.07
2	0.02	0.24	17.3	1.26	0.07	4.59	1.32	3.09	1.50	6.72	1.16	5.21	0.03	0.10
3	0.01	0.09	20.8	0.92	0.07	3.95	0.85	1.58	0.78	4.27	0.78	3.86	0.04	0.08
4	0.03	0.17	15.6	1.30	0.09	4.95	1.03	1.15	0.87	6.50	1.34	2.99	0.06	0.14
5	0.01	0.31	65.1	1.76	0.12	8.29	1.85	1.48	1.23	12.5	1.62	4.40	0.07	0.22
6	0.02	0.23	9.11	0.83	0.08	4.79	1.34	1.12	0.75	5.53	0.92	3.57	0.06	0.17
7	0.02	0.11	13.6	0.93	0.03	5.50	1.87	0.53	0.59	4.69	0.83	2.00	0.02	0.04
8	0.02	0.09	7.85	0.57	0.02	3.11	0.38	1.23	0.69	2.11	0.50	3.03	0.01	0.05
9	0.21	0.05	1.38	0.08	0.01	0.52	0.18	0.40	0.16	0.94	0.88	0.47	0.01	0.01
10	0.05	0.04	8.51	0.39	0.03	1.21	0.47	0.51	0.33	1.76	0.30	1.16	0.02	0.06
11	0.19	0.02	2.17	0.09	0.01	0.35	0.12	0.30	0.16	0.61	0.09	0.14	0.01	0.00
12	4.58	0.03	0.69	0.14	0.01	0.38	0.15	0.38	0.11	0.35	0.13	0.08	0.01	0.01
13	0.27	0.11	18.1	0.55	0.04	1.79	0.72	1.85	0.33	3.01	0.30	2.91	0.01	0.02
14	0.02	0.09	14.9	0.65	0.03	2.75	1.37	5.14	0.43	2.34	0.51	1.87	0.01	0.04
#	#	#	#	#	#	#	#	#	#	#	#	#	#	#
1	246	125	257	245	256	126	126	102	8	126	257	126	257	257
2	182	8	183	171	183	8	8	8	8	8	183	8	183	182
3	185	11	185	173	185	8	8	8	8	8	185	8	185	185
4	183	8	65	53	183	8	8	8	8	8	183	8	90	183
5	255	8	232	233	256	8	8	8	8	103	256	103	199	256
6	179	8	81	69	199	8	8	8	8	23	190	23	90	190
7	211	8	221	211	223	28	28	8	8	8	223	8	221	221
8	176	8	176	176	164	8	8	8	8	8	176	8	176	175
9	55	54	8	8	8	8	8	8	8	9	9	8	8	7
10	222	8	234	222	234	8	8	8	8	8	234	8	234	229
11	8	8	8	8	8	8	8	8	8	8	8	8	8	4
12	68	8	73	68	73	8	8	8	8	8	73	8	73	70
13	259	116	259	247	259	116	116	104	8	116	259	116	259	254
14	259	32	259	247	259	32	32	32	8	7	258	31	259	253

All values are based on data from 2000 to 2022, though their monitoring periods differ.

Table A4. Average DOM characteristics at each site, along with its standard deviation and the amount of data for each parameter and site.

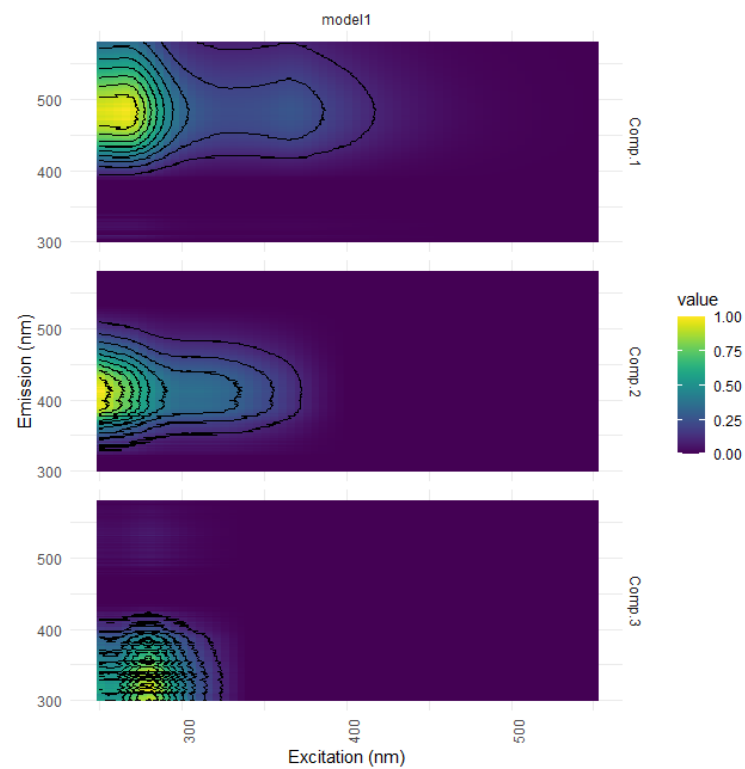
Sort	DOC	sUVa	BOD <sub>5</sub>	COD <sub>Cr</sub>	COD <sub>Mn</sub>	Chl-a	BIX	FI	HIX	VHA	SHA	CHA	NEU	HPO	HPI
#	mg L <sup>-1</sup>	cm <sup>-1</sup> /mg C/L	mg L <sup>-1</sup>	mg L <sup>-1</sup>	mg L <sup>-1</sup>	mg L <sup>-1</sup>				%	%	%	%	%	%
1	6.94	0.033	2.92	21.0	7.65	13.6	0.81	1.29	0.84	71.1	2.72	4.59	21.6	73.8	26.21
2	9.52	0.028	3.62	25.7	7.32	44.1	0.86	1.33	0.84	69.4	7.16	4.80	18.6	76.6	23.4
3	4.87	0.031	2.47	16.2	4.73	6.05	0.87	1.34	0.85	69.0	3.92	0.79	26.3	73.0	27.0
4	6.44	0.028	2.43	19.2	5.99	9.83	0.88	1.37	0.88	69.3	5.21	5.88	19.9	74.5	25.5
5	8.77	0.025	4.07	28.7	8.44	22.1	0.92	1.38	0.84	58.2	16.3	8.47	17.0	74.5	25.5
6	4.78	0.030	2.96	17.3	-	6.21	0.86	1.33	0.85	60.5	11.4	4.05	24.0	71.9	28.1
7	5.43	0.032	2.13	13.4	4.26	3.39	0.83	1.33	0.84	63.2	11.2	0.96	24.6	74.5	25.5
8	2.60	0.031	1.74	8.68	2.93	3.28	0.85	1.32	0.82	54.0	13.4	0.00	32.6	67.4	32.6
9	5.25	0.048	-	-	6.47	-	0.60	1.11	0.86	77.9	5.38	1.13	15.6	83.3	16.7
10	3.59	0.029	1.70	10.3	3.87	-	0.71	1.20	0.84	67.7	3.28	1.25	27.8	71.0	29.0
11	7.03	0.052	-	-	-	-	0.56	1.10	0.87	80.2	4.53	0.72	14.6	84.7	15.3
12	9.49	0.051	1.66	26.3	12.6	-	0.53	1.07	0.87	81.5	6.45	1.60	10.4	88.0	12.0
13	4.05	0.037	1.51	13.7	4.92	-	0.71	1.24	0.87	69.0	6.98	1.80	22.2	76.0	24.0
14	5.53	0.039	1.72	15.8	5.33	3.07	0.69	1.21	0.88	68.9	10.2	3.18	17.7	79.1	20.9

Table A4. Cont.

Sort	DOC	sUVa	BOD <sub>5</sub>	COD <sub>Cr</sub>	COD <sub>Mn</sub>	Chl-a	BIX	FI	HIX	VHA	SHA	CHA	NEU	HPO	HPI	
#	mg L <sup>-1</sup>	cm <sup>-1</sup> / mg C/L)	mg L <sup>-1</sup>	mg L <sup>-1</sup>	mg L <sup>-1</sup>	mg L <sup>-1</sup>				%	%	%	%	%	%	
	STD	STD	STD	STD	STD	STD	STD	STD	STD	STD	STD	STD	STD	STD	STD	STD
1	2.60	0.01	1.08	8.80	3.58	10.4	0.06	0.05	0.04	6.32	3.32	5.30	10.29	6.31	6.31	
2	4.15	0.01	1.39	9.13	2.50	27.4	0.06	0.04	0.03	5.76	4.80	5.64	7.57	5.40	5.40	
3	1.22	0.00	1.33	8.22	1.82	7.28	0.04	0.03	0.03	3.31	7.84	1.59	7.23	5.73	5.73	
4	1.49	0.00	1.39	9.00	1.83	7.01	0.04	0.03	0.02	6.97	7.02	4.50	6.62	7.43	7.43	
5	2.16	0.00	2.25	22.5	2.86	20.4	0.03	0.03	0.03	3.59	3.22	3.87	5.30	3.89	3.89	
6	1.18	0.00	1.50	6.58	-	7.40	0.04	0.03	0.03	4.35	8.20	5.06	11.9	7.32	7.32	
7	1.98	0.00	0.83	7.16	2.36	3.21	0.03	0.04	0.06	2.01	7.79	1.11	9.56	8.69	8.69	
8	0.94	0.00	0.70	4.09	1.75	1.65	0.06	0.06	0.06	8.52	9.90	0.00	12.9	12.9	12.9	
9	3.18	0.00	-	-	4.43	-	0.04	0.04	0.07	6.18	4.72	2.27	5.24	3.81	3.81	
10	1.52	0.01	0.91	6.56	2.51	-	0.06	0.04	0.07	12.1	4.12	2.49	15.2	13.3	13.3	
11	5.69	0.00	-	-	-	-	0.03	0.03	0.05	10.1	2.65	0.52	10.8	10.5	10.5	
12	5.84	0.00	0.72	14.4	7.07	-	0.03	0.02	0.05	6.45	3.12	1.87	9.87	9.32	9.32	
13	2.35	0.00	1.09	14.7	4.08	-	0.04	0.04	0.04	7.40	4.82	3.61	14.7	11.7	11.7	
14	2.53	0.00	0.97	9.41	3.15	3.64	0.02	0.03	0.03	3.77	7.28	3.72	7.38	6.34	6.34	
	#	#	#	#	#	#	#	#	#	#	#	#	#	#	#	
1	209	8	247	249	236	214	8	8	8	4	4	4	4	4	4	
2	8	8	173	175	9	11	8	8	8	4	4	4	4	4	4	
3	8	8	176	177	45	132	8	8	8	4	4	4	4	4	4	
4	8	8	165	175	45	29	8	8	8	4	4	4	4	4	4	
5	8	8	247	248	120	29	8	8	8	4	4	4	4	4	4	
6	8	8	145	182	0	29	8	8	8	4	4	4	4	4	4	
7	18	8	213	215	96	40	8	8	8	4	4	4	4	4	4	
8	8	8	167	168	96	6	8	8	8	4	4	4	4	4	4	
9	9	8	0	0	47	0	8	8	8	4	4	4	4	4	4	
10	78	114	223	226	213	0	8	8	8	4	4	4	4	4	4	
11	8	8	0	0	0	0	8	8	8	4	4	4	4	4	4	
12	49	8	65	65	59	0	8	8	8	4	4	4	4	4	4	
13	92	7	249	251	238	0	8	8	8	4	4	4	4	4	4	
14	104	8	250	251	120	84	8	8	8	4	4	4	4	4	4	

DOC and sUVa are based on data from 2000 to 2022; BOD<sub>5</sub>, COD<sub>Cr</sub>, COD<sub>Mn</sub>, and Chl-a are based on data from 2000 to 2020; while HIX, FI, and HIX are from 2020 to 2022. DOM fractions are based on half of the samples from 2020 to 2022.

## Appendix C



**Figure A1.** Counterplots of the fluorescence intensity by excitation wavelength (nm,  $x$ -axis) and emission wavelength (nm,  $y$ -axis) of the three modelled PARAFAC components, Component 1 (Comp. 1), Component 2 (Comp. 2), and Component 3 (Comp. 3).

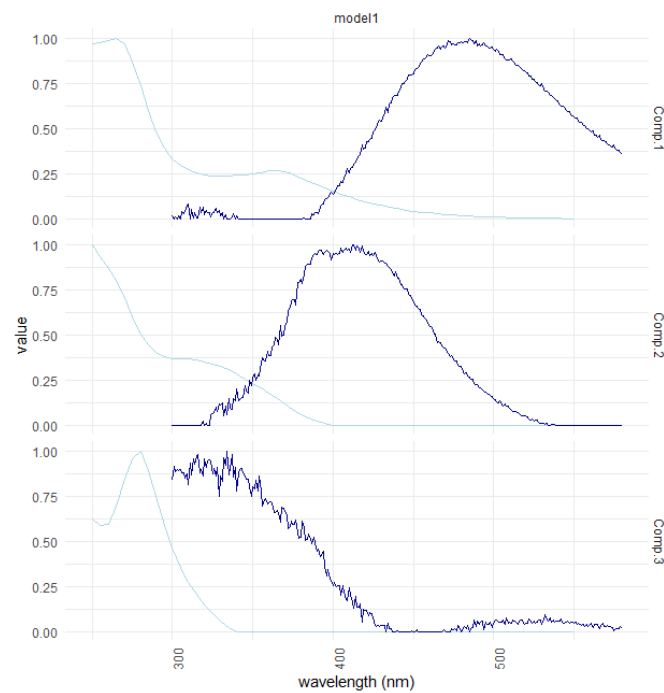


**Figure A2.** Spectral loadings of the three-component PARAFAC model. Excitation wavelengths in light blue and emission wavelengths in dark blue.

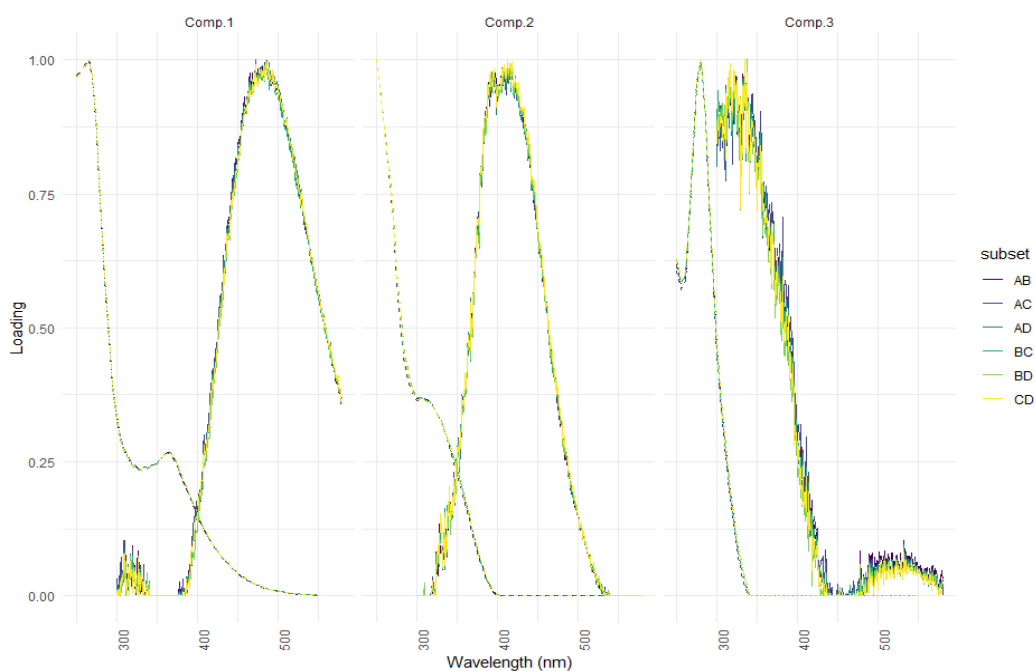


**Figure A3.** Loadings from the split-half analysis of the PARAFAC model with three components. Model validation test.

**Table A5.** List of studies from the OpenFluor database with components matching (>0.95) the excitation and emission of the components found in the study. The ten studies presented for each component were selected among the strongest correlating, readily available, and by prioritizing studies that matched more than one of the three components in this study. For component assignment and description, the reader is referred also to the references within the cited studies.

Ref.	Component Assignment and Description	Location	Sample Type	Excitation/Emission Similarity Score
Component 1: $\lambda_{excitation, max}/\lambda_{emission, max} = 265 (365)/487$				
1	[43] RaskaDOM C2: Humic-like; large-sized; characteristics of soil, sediment, and freshwater environments.	Cropping system, Montana, USA	Soil water extractable DOM	0.9920/0.9946
2	[64] Wheat C2: Humic-like; large-sized; characteristics of soil, sediment, and freshwater environments.	Cropping system, Montana, USA	Soil water extractable DOM	0.9876/0.9972
3	[65] Recycle C1: Terrestrial humic-like fluorescence in high nutrient and wastewater-impacted environments.	Water recycling plant, Australia	Water recycling DOM	0.9808/0.9986
4	[66] Galveston bay C1: similar to Coble peak C; humic-like.	Texas, USA	Riverine/Estuarine DOM	0.9802/0.9975
5	[67] Gueguen_Nelson C1: Humic-like; terrestrially derived; Coble peak C; some photobleaching.	Beaufort Sea, experiments	Estuarine DOM	0.9792/0.9933
6	[68] Macaronesia C3: humic-like.	Sao Vicente, Cape Verde, to Gran Canaria, Canary Island	Marine DOM	0.9753/0.9968



Table A5. Cont.

Ref.	Component Assignment and Description	Location	Sample Type	Excitation/Emission Similarity Score
7	[69] C1: Coble peak C+A; Humic-like; terrestrially derived.	Australia	Water treatment plant DOM	0.9723/0.9988
8	[43] C2: humic-like; terrestrially derived material identified in a variety of aquatic environments; photosensitive.	Various freshwater environments across Quebec, Canada	Boreal freshwater DOM	0.9965/0.9728
9	[40] C1: terrestrial and marine DOM.	Fjordsystem, Norway	Experimental marine DOM	0.9798/0.9861
10	[41] C2: aromatic; high molecular weight organic matter (humic-like) with terrestrial character and correlated to lignin phenol concentrations; humic-like substance, enriched in terrestrial DOM sources; ubiquitous in DOM.	Experiments	SRHA DOM standard from the International Humic Substances Society	0.9832/0.9724
Component 2: $\lambda_{excitation, max}/\lambda_{emission, max} = 250\ 305/413$				
1	[70] C4: UVA humic-like component frequently found in lentic freshwater; associated with bacterial planktonic activity.	The Sau Reservoir and its tributary the Ter River, Spain	Freshwater DOM	0.9823/0.9924
2	[41] C3: combined Coble peaks A+M; microbial humic-like substances; produced by microbial degradation of organic matter.	Experiments	SRHA DOM standard from the International Humic Substances Society	0.9887/0.9842
3	[67] C2: Humic-like; terrestrially derived; Coble peak A; susceptible to photobleaching.	Beaufort Sea, experiments	Estuarine DOM	0.9790/0.9898
4	[44] C2: humic-like, ubiquitous humic component related with fulvic acids and re-processed humics.	Montseny Natural Park, Spain	Headwater forested catchment freshwater DOM	0.9717/0.9968
5	[45] C1: terrestrial humic-like, microbial-humic-like.	The Baltimore sewer system, Baltimore, USA	Wastewater DOM	0.9810/0.9865
6	[66] Galveston bay C2: similar to Coble peak M.	Texas, USA	Riverine/Estuarine DOM	0.9834/0.9826
7	[69] C2: Coble peaks C+A; humic-like; terrestrial delivered reprocessed OM.	Australia	Water treatment plant DOM	0.9733/0.9886
8	[43] C1: Humic-like; medium sized; characteristics of soil, sediment, and freshwater environments.	Cropping system, Montana, USA	Soil water extractable DOM	0.9718/0.9548
9	[64] C2: Humic-like; medium sized; characteristics of soil, sediment, and freshwater environments.	Cropping system, Montana, USA	Soil water extractable DOM	0.9826/0.9761
10	[65] C2: Microbial humic-like.	Water recycling plant, Australia	Water recycling DOM	0.9826/0.9679

Table A5. Cont.

Ref.	Component Assignment and Description	Location	Sample Type	Excitation/Emission Similarity Score
Component 3: $\lambda_{excitation, max}/\lambda_{emission, max} = 280/336$				
1	[71] C7: Protein-like; both tyrosine- and tryptophan-like properties.	Southern Ontario, Canada	Stormwater pond DOM	0.9951/0.9961
2	[72] C5: Coble peak T; tryptophan-like.	Mackenzie, Lena, Kolyma, Ob, and Yenisei Rivers	Arctic river DOM	0.9878/0.9947
3	[73] C5: Coble T peak; protein-like/tryptophan-like material with a recent, probably microbial origin.	Drinking water treatment plant, Sweden	Drinking water treatment plant water DOM	0.9935/0.9867
4	[74] C2: tryptophan-like; protein-like.	Maryland, USA	Leaf litter leachate	0.9877/0.9924
5	[69] C4: Coble peaks T+B, protein-like; microbial delivered.	Australia	Water treatment plant DOM	0.9885/0.9886
6	[46] C4: tryptophan-like and protein-like material; generally contributes the highest intensity peaks in wastewaters, even in treated effluents; indicates recent production; often found in anthropogenically affected watersheds.	Coastal drainage basins of Miami, FL, USA	Coastal DOM	0.9913/0.9845
7	[75] C3: Protein-like; fresh production; biological production; higher in surface water layer.	Indian ocean	Marine DOM	0.9978/0.9781
8	[76] C4: Tryptophan-like; both photodegraded and produced during photodegradation, depending on sample type.	Subtropical Minjiang watershed, China	Wastewater, leaf litter leachates, river water DOM	0.9864/0.9836
9	[42] C6: Associated with freshly produced protein-like material; tryptophan-like; strongest predictor of BDOC.	Various freshwater environments across Quebec, Canada	Boreal freshwater DOM	0.9663/0.9825
10	[45] C4: Tryptophan-like; wastewater indicator.	The Baltimore sewer system, Baltimore, USA	Wastewater DOM	0.9953/0.9538

Appendix D

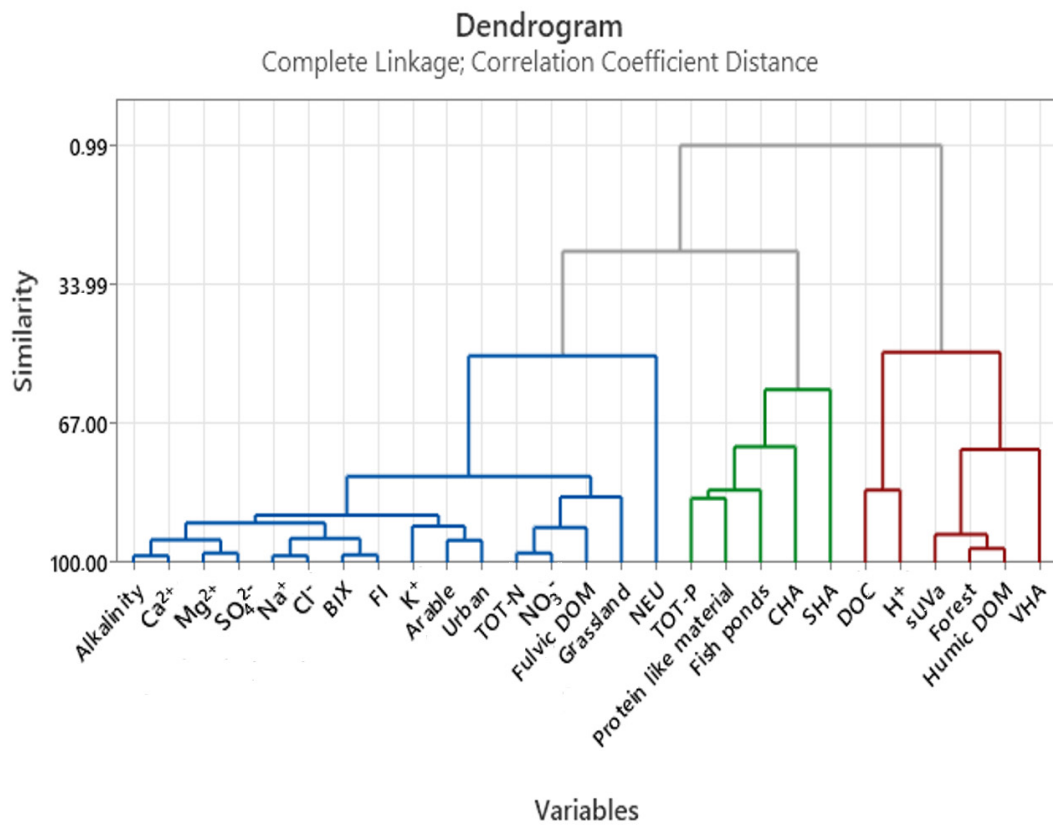


**Figure A4.** Cluster analysis of the water chemistry, sUVa, and catchment land use, along with the three PARAFAC component groups and DOM fractions on half of the quarterly data from 2021 to 2022.

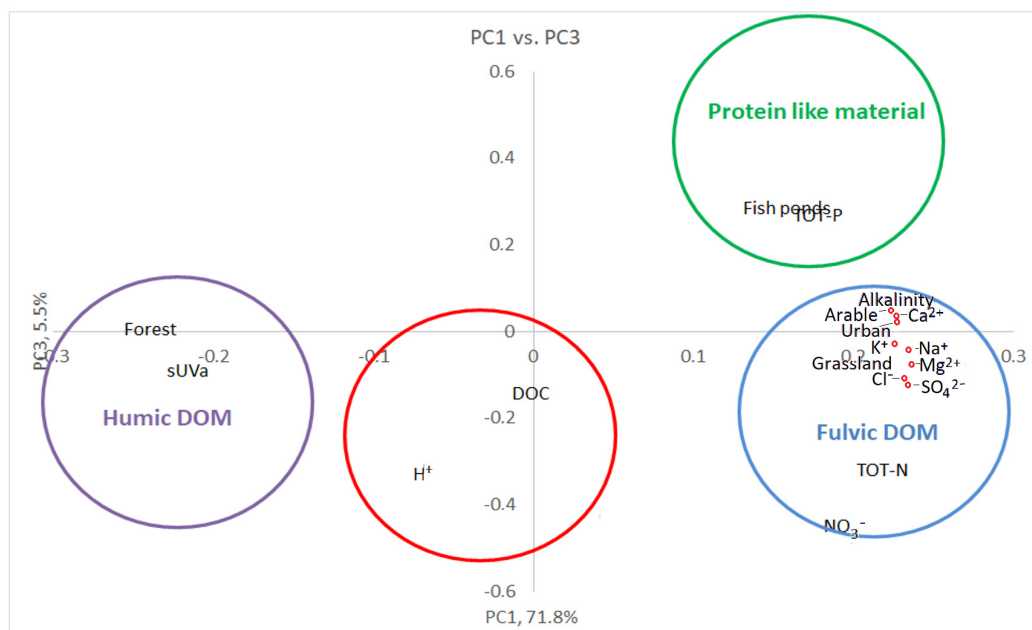


**Figure A5.** The 1<sup>st</sup> and 3<sup>rd</sup> Principal Component (PC) from a Principal Component Analysis of the three PARAFAC component groups, catchment characteristics, and water chemistry on the quarterly data from 2021 to 2022.

## References

1. Thurman, E.M. *Organic Geochemistry of Natural Waters*; Springer: Dordrecht, The Netherlands, 1985. [CrossRef]
2. Chudoba, J.; Hejzlar, J.; Doležal, M. Microbial polymers in the aquatic environment—III. Isolation from river, potable and ground water and analysis. *Water Res.* **1986**, *20*, 1223–1227. [CrossRef]
3. Perdue, E.M. Natural Organic matter. In *Reference Module in Earth Systems and Environmental Sciences, from Encyclopedia of Inland Waters*; Likens, G.E., Ed.; Elsevier: Amsterdam, The Netherlands, 2009. [CrossRef]
4. Swyngedouw, E. Modernity and Hybridity: Nature, Regeneracionismo, and the Production of the Spanish Waterscape, 1890–1930. *Ann. Assoc. Am. Geogr.* **1999**, *89*, 443–465. [CrossRef]
5. Scholz, R.W. *Environmental Literacy in Science and Society; From Knowledge to Decisions*; Cambridge University Press: Cambridge, UK, 2011.
6. Moore, J.W. *Capitalism in the Web of Life*; Verso: London, UK, 2015.
7. Bonneuil, C.; Fressoz, J.-B. *The Shock of the Anthropocene*; Verso: London, UK, 2017.
8. Winter, K.B.; Lincoln, N.K.; Berkes, F. The Social-Ecological Keystone Concept: A Quantifiable Metaphor for Understanding the Structure, Function, and Resilience of a Biocultural System. *Sustainability* **2018**, *10*, 3294. [CrossRef]
9. Hejzlar, J.; Chudoba, J. Microbial polymers in the aquatic environment—II. Isolation from biologically non-purified and purified municipal waste water and analysis. *Water Res.* **1986**, *20*, 1217–1221. [CrossRef]
10. Monteith, D.T.; Stoddard, J.L.; Evans, C.D.; De Wit, H.A.; Forsius, M.; Høgåsen, T.; Wilander, A.; Skjelkvåle, B.L.; Jeffries, D.S.; Vuorenmaa, J.; et al. Dissolved organic carbon trends resulting from changes in atmospheric deposition chemistry. *Nature* **2007**, *450*, 537–540. [CrossRef] [PubMed]
11. De Wit, H.A.; Mulder, J.; Hindar, A.; Hole, L. Long-term increase in dissolved organic carbon in streamwaters in Norway is responsible to reduced acid deposition. *Environ. Sci. Technol.* **2007**, *41*, 7706–7713. [CrossRef]
12. Monteith, D.T.; Henrys, P.A.; Hruška, J.; de Wit, H.A.; Krám, P.; Moldan, F.; Posch, M.; Ráike, A.; Stoddard, J.L.; Shilland, E.M.; et al. Long-term rise in riverine dissolved organic carbon concentration is predicted by electrolyte solubility theory. *Sci. Adv.* **2023**, *9*, eade3491. [CrossRef] [PubMed]
13. Vogt, R.D.; de Wit, H.; Koponen, K. Case Study on Impacts of Large-Scale Re-/Afforestation on Ecosystem Services in Nordic Regions. Report Series Quantifying and Deploying Responsible Negative Emissions in Climate Resilient Pathways. Horizon 2020, Grant Agreement no. 869192. 2022. Available online: [https://www.negemproject.eu/wp-content/uploads/2022/06/NEGEM\\_D3.6\\_Case-study-on-impacts-of-large-scale-re-afforestation-on-ecosystem-services-in-Nordic-regions.pdf](https://www.negemproject.eu/wp-content/uploads/2022/06/NEGEM_D3.6_Case-study-on-impacts-of-large-scale-re-afforestation-on-ecosystem-services-in-Nordic-regions.pdf) (accessed on 17 August 2023).
14. Kopáček, J.; Evans, C.D.; Hejzlar, J.; Kaňa, J.; Porcal, P.; Šantrůčková, H. Factors affecting the leaching of dissolved organic carbon after tree dieback in an unmanaged European mountain forest. *Environ. Sci. Technol.* **2018**, *52*, 6291–6299. [CrossRef]
15. De Wit, H.A.; Garmo, Ø.A.; Jackson-Blake, L.; Clayer, F.; Vogt, R.D.; Kaste, Ø.; Gundersen, C.B.; Guerrerro, J.L.; Hindar, A. Changing Water Chemistry in One Thousand Norwegian Lakes During Three Decades of Cleaner Air and Climate Change. *Glob. Biogeochem. Cycles* **2023**, *37*, e2022GB007509. [CrossRef]
16. Madsen, H.; Lawrence, D.; Lang, M.; Martinkova, M.; Kjeldsen, T.R. Review of trend analysis and climate change projections of extreme precipitation and floods in Europe. *J. Hydrol.* **2014**, *519*, 3634–3650. [CrossRef]
17. Grennfelt, P.; Engleryd, A.; Forsius, M.; Hov, Ø.; Rodhe, H.; Cowling, E. Acid rain and air pollution: 50 years of progress in environmental science and policy. *Ambio* **2020**, *49*, 849–864. [CrossRef]
18. Schulte-Uebbing, L.; de Vries, W. Global-scale impacts of nitrogen deposition on tree carbon sequestration in tropical, temperate, and boreal forests: A meta-analysis. *Glob. Chang. Biol.* **2018**, *24*, 416–431. [CrossRef]
19. Kaste, Ø.; Skarbøvik, E.; Vogt, R.D. Assessment of Parameters for Suspended Solids and Organic Matter Can Be Included in the Water Classification System (in Norwegian). NIVA-Rapport 7860. 2023. Available online: <https://hdl.handle.net/11250/3067437> (accessed on 17 August 2023).
20. Hansen, A.M.; Kraus, T.E.C.; Pellerin, B.A.; Fleck, J.A.; Downing, B.D.; Bergamaschi, B.A. Optical properties of dissolved organic matter (DOM): Effects of biological and photolytic degradation. *Limnol. Oceanogr.* **2016**, *61*, 1015–1032. [CrossRef]
21. Sample, J.E.; Jackson-Blake, L.; Vogelsang, C.; Kaste, Ø.; Vogt, R.D. TEOTIL3: A coefficient-based export model for simulation of river inputs (in Norwegian). NIVA report. In Prep. 2023. Available online: <https://niva.brage.unit.no/niva-xmlui/> (accessed on 17 August 2023).
22. Zsolnay, A.; Baigar, E.; Jimenez, M.; Steinweg, B.; Saccomandi, F. Differentiating with fluorescence spectroscopy the sources of dissolved organic matter in soils subjected to drying. *Chemosphere* **1999**, *38*, 45–50. [CrossRef] [PubMed]
23. Huguet, A.; Vacher, L.; Relexans, S.; Saubusse, S.; Froidefond, J.M.; Parlanti, E. Properties of fluorescent dissolved organic matter in the Gironde Estuary. *Org. Geochem.* **2009**, *40*, 706–719. [CrossRef]
24. Murphy, K.R.; Stedmon, C.A.; Wenig, P.; Bro, R. OpenFluor— an online spectral library of auto-fluorescence by organic compounds in the environment. *Anal. Methods* **2014**, *6*, 658–661. [CrossRef]
25. Xu, X.; Kang, J.; Shen, J.; Zhao, S.; Wang, B.; Zhang, X.; Chen, Z. EEM-PARAFAC characterization of dissolved organic matter and its relationship with disinfection by-products formation potential in drinking water sources of northeastern China. *Sci. Total Environ.* **2021**, *774*, 145297. [CrossRef]

26. Vogt, R.D.; Akkanen, J.; Andersen, D.O.; Bruggemann, R.; Chatterjee, B.; Gjessing, E.; Kukkonen, J.V.K.; Larsen, H.E.; Luster, J.; Paul, A.; et al. Key site variables governing the functional characteristics of dissolved natural organic matter (DNOM) in Nordic forested catchments. *Aquat. Sci.* **2004**, *66*, 195–210. [[CrossRef](#)]
27. Mykkelbost, T.C.; Vogt, R.D.; Seip, H.M.; Riise, G. Organic carbon fractionation applied to lake-and soil water at the HUMEX site. *Environ. Int.* **1995**, *21*, 849–859. [[CrossRef](#)]
28. Kopáček, J.; Hejzlar, J.; Porcal, P.; Posh, M. Trends in riverine element fluxes: A chronicle of regional socio-economic changes. *Water Res.* **2017**, *125*, 374–383. [[CrossRef](#)]
29. Veselý, J.; Hruška, J.; Norton, S.A.; Johnson, C.E. Trends in water chemistry of acidified Bohemian lakes from 1984 to 1995: I. Major solutes. *Water Air Soil Pollut.* **1998**, *108*, 107–127. [[CrossRef](#)]
30. Carlson, M. Mapping of Causes for Increase in Dissolved Organic Matter in a Czech Watershed. Master Thesis, University of Oslo, Oslo, Norway, June 2021. Available online: <https://www.duo.uio.no/handle/10852/93531> (accessed on 17 August 2023).
31. Schmidt, S.I.; Hejzlar, J.; Kopáček, J.; Paule-Mercado, M.C.; Porcal, P.; Vystavna, Y.; Lanta, V. Forest damage and subsequent recovery alter the water composition in mountain lake catchments. *Sci. Total Environ.* **2022**, *827*, 154293. [[CrossRef](#)]
32. Chow, C.W.K.; Fabris, R.; Drikas, M. A rapid fractionation technique to characterise natural organic matter for the optimisation of water treatment processes. *J. Water Supply Res. Technol. AQUA* **2004**, *53*, 85–92. [[CrossRef](#)]
33. Ohno, T. Fluorescence Inner-Filtering Correction for Determining the Humification Index of Dissolved Organic Matter. *Environ. Sci. Technol.* **2002**, *36*, 742–746. [[CrossRef](#)]
34. Fellman, J.B.; Hood, E.; Spencer, R.G.M. Fluorescence Spectroscopy Opens New Windows into Dissolved Organic Matter Dynamics in Freshwater Ecosystems: A Review. *Limnol. Oceanogr.* **2010**, *55*, 2452–2462. [[CrossRef](#)]
35. Li, P.; Hur, J. Utilization of UV-Vis spectroscopy and related data analyses for dissolved organic matter (DOM) studies: A review. *Critical Reviews in Environ. Sci. Technol.* **2017**, *47*, 131–154. [[CrossRef](#)]
36. McKnight, D.M.; Boyer, E.W.; Westerhoff, P.K.; Doran, P.T.; Kulbe, T.; Andersen, D.T. Spectrofluorometric Characterization of Dissolved Organic Matter for Indication of Precursor Organic Material and Aromaticity. *Limnol. Oceanogr.* **2001**, *46*, 38–48. [[CrossRef](#)]
37. da Silva, M.P.; Sander de Carvalho, L.A.; Novo, E.; Jorge, D.S.F.; Barbosa, C.C.F. Use of optical absorption indices to assess seasonal variability of dissolved organic matter in Amazon floodplain lakes. *Biogeosciences* **2020**, *17*, 5355–5364. [[CrossRef](#)]
38. Pucher, M.; Wunsch, U.; Weigelhofer, G.; Murphy, K.; Hein, T.; Graeber, D. staRdom: Versatile Software for Analyzing Spectroscopic Data of Dissolved Organic Matter in R'. *Water* **2019**, *11*, 2366. [[CrossRef](#)]
39. R Core Team. *R: A Language and Environment for Statistical Computing*; R Foundation for Statistical Computing: Vienna, Austria, 2023; Available online: <https://www.R-project.org/> (accessed on 15 July 2023).
40. Stedmon, C.; Bro, R. Characterizing Dissolved Organic Matter Fluorescence with Parallel Factor Analysis: A Tutorial. *Limnol. Oceanogr.* **2008**, *6*, 572–579. [[CrossRef](#)]
41. Du, Y.; Zhang, Q.; Liu, Z.; He, H.; Lürling, M.; Chen, M.; Zhang, Y. Composition of dissolved organic matter controls interactions with La and Al ions: Implications for phosphorus immobilization in eutrophic lakes. *Environ. Pollut.* **2019**, *248*, 36–47. [[CrossRef](#)] [[PubMed](#)]
42. Lapiere, J.F.; del Giorgio, P.A. Partial coupling and differential regulation of biologically and photochemically labile dissolved organic carbon across boreal aquatic networks. *Biogeosciences* **2014**, *11*, 5969–5985. [[CrossRef](#)]
43. Romero, C.M.; Engel, R.E.; D'Andrilli, J.; Miller, P.R.; Wallander, R. Compositional tracking of dissolved organic matter in semiarid wheat-based cropping systems using fluorescence EEMs-PARAFAC and absorbance spectroscopy. *J. Arid. Environ.* **2019**, *167*, 34–42. [[CrossRef](#)]
44. Bernal, S.; Lupon, A.; Catalán, N.; Castelar, S.; Martí, E. Decoupling of dissolved organic matter patterns between stream and riparian groundwater in a headwater forested catchment. *Hydrol. Earth Syst. Sci.* **2018**, *22*, 1897–1910. [[CrossRef](#)]
45. Batista-Andrade, J.A.; Diaz, E.; Iglesias Vega, D.; Hain, E.; Rose, M.R.; Blaney, L. Spatiotemporal analysis of fluorescent dissolved organic matter to identify the impacts of failing sewer infrastructure in urban streams. *Water Res.* **2023**, *229*, 119521. [[CrossRef](#)]
46. Smith, M.A.; Kominoski, J.S.; Gaiser, E.E.; Price, R.M.; Troxler, T.G. Stormwater Runoff and Tidal Flooding Transform Dissolved Organic Matter Composition and Increase Bioavailability in Urban Coastal Ecosystems. *J. Geophys. Res. B* **2021**, *126*, e2020JG006146. [[CrossRef](#)]
47. Eikebrokk, B.; Haaland, S.L.; Jarvis, P.; Riise, G.; Vogt, R.D.; Zahlsen, K. NOMiNOR: Natural Organic Matter in Drinking Waters within the Nordic Region. In *Norsk Vann Report*; Norwegian Water: Oslo, Norway, 2018; Volume 231, Available online: <https://va-kompetanse.no/butikk/a-231-nominor-natural-organic-matter-in-drinking-waters-within-the-nordic-region-kun-digital/> (accessed on 17 August 2023).
48. Crapart, C.; Andersen, T.; Hessen, D.O.; Valiente, N.; Vogt, R.D. Factors Governing Biodegradability of Dissolved Natural Organic Matter in Lake Water. *Water* **2021**, *13*, 2210. [[CrossRef](#)]
49. Crapart, C.; Finstad, A.G.; Hessen, D.O.; Vogt, R.D.; Andersen, T. Spatial predictors and temporal forecast of total organic carbon levels in boreal lakes. *Sci. Total Environ.* **2023**, *870*, 161676. [[CrossRef](#)]



50. ČSN EN 12880; Water Quality, Determination of Dry Residue and Water Content of Sludges and Sludge Products. Czech Office for Standards, Metrology and Testing: Prague, Czech Republic, 2000.
51. ČSN EN ISO 9963-1; Water Quality. Determination of Alkalinity. Part 1: Determination of Total and Composite Alkalinity. Czech Office for Standards, Metrology and Testing: Prague, Czech Republic, 1995.
52. ČSN EN ISO 5815-1; Water Quality—DETERMINATION of Biochemical Oxygen Demand After n Days (BOD<sub>n</sub>)—Part 1: Dilution and Seeding Method with Allylthiourea Addition. Czech Office for Standards, Metrology and Testing: Prague, Czech Republic, 2020.
53. ČSN EN ISO 8467; Water Quality—Determination of Chemical Oxygen Demand by Permanganate (CODMn). Czech Office for Standards, Metrology and Testing: Prague, Czech Republic, 1997.
54. ČSN ISO 157085; Geometrical Product Specifications (GPS)—Surface Texture: Profile Method—Terms, Definitions and Surface Texture Parameters. Czech Office for Standards, Metrology and Testing: Prague, Czech Republic, 2008.
55. ČSN 757360; Water Quality, Determination of Absorbance. Direct Measurement of Absorption of UV Radiation at Wavelength 254 nm. Czech Office for Standards, Metrology and Testing: Prague, Czech Republic, 2013.
56. ISO 17294-2; Water Quality-Application of Inductively Coupled Plasma Mass Spectrometry (ICP-MS)-Part 2: Determination of 62 Elements. International Organization for Standardization (ISO): Geneva, Switzerland, 2003; Volume 2.
57. ISO 6878; Water Quality—Determination of Phosphorus—Ammonium Molybdate Spectrometric Method. International Organization for Standardization (ISO): Geneva, Switzerland, 2004.
58. DIN EN 12260; Water Quality. Determination of Nitrogen. Determination of Bound Nitrogen (TN<sub>b</sub>), following Oxidation to Nitrogen Oxides. Deutsches Institut für Normung: Berlin, Germany, 2003.
59. ISO 7150-1; Water Quality-Determination of Ammonium. Part 1: Manual Spectrometric Method. International Organization for Standardization (ISO): Geneva, Switzerland, 1984.
60. ISO10304-1; Water Quality-Determination of Dissolved Anions by Liquid Chromatography of Ions-Part 1: Determination of Bromide, Chloride, Fluoride, Nitrate, Nitrite, Phosphate and Sulfate. International Organization for Standardization (ISO): Geneva, Switzerland, 2007; Volume 1.
61. ČSN EN ISO 14911; Water Quality—Determination of Dissolved Li<sup>+</sup>, Na<sup>+</sup>, NH<sub>4</sub><sup>+</sup>, K<sup>+</sup>, Mn<sup>2+</sup>, Ca<sup>2+</sup>, Mg<sup>2+</sup>, Sr<sup>2+</sup> and Ba<sup>2+</sup> Using Ion Chromatography—Method for Water and Waste Water. Czech Office for Standards, Metrology and Testing: Prague, Czech Republic, 2000.
62. ISO 10260; Water Quality, Measurement of Biochemical Parameters; Spectrometric Determination of Chlorophyll-a Concentration (ISO: 1992). International Organization for Standardization (ISO): Geneva, Switzerland, 1992.
63. ISO 8245; Water Quality-Guidelines for the Determination of Total Organic Carbon (TOC) and Dissolved Organic Carbon (DOC). International Organization for Standardization (ISO): Geneva, Switzerland, 1999.
64. Romero, C.M.; Engel, R.E.; D'Andrilli, J.; Chen, C.; Zabinski, C.; Miller, P.R.; Wallander, R. Bulk optical characterization of dissolved organic matter from semiarid wheat-based cropping systems. *Geoderma* **2017**, *306*, 40–49. [[CrossRef](#)]
65. Murphy, K.R.; Stedmon, C.A.; Graeber, D.; Bro, R. Fluorescence spectroscopy and multi-way techniques. PARAFAC. *Anal. Methods* **2013**, *5*, 6557–6566. [[CrossRef](#)]
66. Gold-Bouchot, G.; Polis, S.; Castañón, L.E.; Flores, M.P.; Alsante, A.N.; Thornton, D.C.O. Chromophoric dissolved organic matter (CDOM) in a subtropical estuary (Galveston Bay, USA) and the impact of Hurricane Harvey. *Environ. Sci. Pollut. Res.* **2021**, *28*, 53045–53057. [[CrossRef](#)]
67. Guéguen, C.; Mokhtar, M.; Perroud, A.; McCullough, G.; Papakyriakou, T. Mixing and photoreactivity of dissolved organic matter in the Nelson/Hayes estuarine system (Hudson Bay, Canada). *J. Mar. Syst.* **2016**, *161*, 42–48. [[CrossRef](#)]
68. Santana-Casiano, J.M.; González-Santana, D.; Devresse, Q.; Hepach, H.; Santana-González, C.; Quack, B.; Engel, A.; González-Dávila, M. Exploring the Effects of Organic Matter Characteristics on Fe(II) Oxidation Kinetics in Coastal Seawater. *Environ. Sci. Technol.* **2022**, *56*, 2718–2728. [[CrossRef](#)] [[PubMed](#)]
69. Shutova, Y.; Baker, A.; Bridgeman, J.; Henderson, R.K. Spectroscopic characterisation of dissolved organic matter changes in drinking water treatment: From PARAFAC analysis to online monitoring wavelengths. *Water Res.* **2014**, *54*, 159–169. [[CrossRef](#)]
70. Marcé, R.; Verdura, L.; Leung, N. Dissolved organic matter spectroscopy reveals a hot spot of organic matter changes at the river–reservoir boundary. *Aquat. Sci.* **2021**, *83*, 67. [[CrossRef](#)]
71. Williams, C.J.; Frost, P.C.; Xenopoulos, M.A. Beyond best management practices: Pelagic biogeochemical dynamics in urban stormwater ponds. *Ecol. Appl.* **2013**, *23*, 1384–1395. [[CrossRef](#)] [[PubMed](#)]
72. Walker, S.A.; Amon, R.M.W.; Stedmon, C.A. Variations in high-latitude riverine fluorescent dissolved organic matter: A comparison of large Arctic rivers. *J. Geophys. Res. Biogeosci.* **2013**, *118*, 1689–1702. [[CrossRef](#)]
73. Moona, N.; Holmes, A.; Wunsch, U.J.; Pettersson, T.J.R.; Murphy, K.R. Full-Scale Manipulation of the Empty Bed Contact Time to Optimize Dissolved Organic Matter Removal by Drinking Water Biofilters. *ACS EST Water* **2021**, *1*, 1117–1126. [[CrossRef](#)]
74. Wheeler, K.I.; Levia, D.F.; Hudson, J.E. Tracking senescence-induced patterns in leaf litter leachate using parallel factor analysis (PARAFAC) modeling and self-organizing maps. *Journal of Geophysical Research. J. Geophys. Res. Biogeosci.* **2017**, *122*, 2233–2250. [[CrossRef](#)]



75. Kim, J.; Kim, Y.; Kang, H.-W.; Kim, S.H.; Rho, T.; Kang, D.-J. Tracing water mass fractions in the deep western Indian Ocean using fluorescent dissolved organic matter. *Mar. Chem.* **2020**, *218*, 103720. [[CrossRef](#)]
76. Zhuang, W.-E.; Chen, W.; Yang, L. Effects of Photodegradation on the Optical Indices of Chromophoric Dissolved Organic Matter from Typical Sources. *Int. J. Environ. Res. Public Health* **2022**, *19*, 14268. [[CrossRef](#)] [[PubMed](#)]

**Disclaimer/Publisher's Note:** The statements, opinions and data contained in all publications are solely those of the individual author(s) and contributor(s) and not of MDPI and/or the editor(s). MDPI and/or the editor(s) disclaim responsibility for any injury to people or property resulting from any ideas, methods, instructions or products referred to in the content.